

Beyond Benchmarks: A Novel Framework for Domain-Specific LLM Evaluation and Knowledge Mapping

Nitin Sharma¹, Thomas Wolfers¹, and Çağatay Yıldız²

¹Department of Psychiatry and Psychotherapy, University of Tübingen

²University of Tübingen

Abstract

The paper addresses two critical challenges in language model (LM) evaluation: creating reliable domain-specific benchmarks and understanding knowledge representation during domain adaptation. We introduce a deterministic pipeline that converts raw domain corpora into completion-type benchmarks without relying on LMs or human curation, eliminating benchmark contamination issues while enabling evaluation on the latest domain data. Our approach generates domain-specific keywords and related word lists using Term Frequency (TF) and Term Frequency-Inverse Document Frequency (TF-IDF) methods and constructs prompt-target pairs. We evaluate models by measuring their ability to complete these prompts with the correct domain-specific targets, providing a direct assessment of domain knowledge with low computational cost. Through comprehensive experiments across multiple models (GPT-2 medium/XL, Llama-2/3.1, OLMo-2, Qwen-2, Mistral) and domains, we demonstrate that our benchmark strongly correlates with expert-generated benchmarks while providing a more accurate measure of domain knowledge than traditional perplexity metrics. We reveal that domain adaptation happens rapidly in smaller models (within 500 steps) and illustrate a new approach to domain knowledge evaluation in base models during training for early stopping. By extending mechanistic analysis to domain adaptation, we discover that initial-to-mid layers are primarily responsible for attribute extraction, while later layers focus on next token prediction. Furthermore, we show that during adaptation, forgetting begins in the middle layers, where attribute extraction happens and is amplified in later layers. Our work provides both a practical evaluation methodology for domain-specific LMs and novel insights into knowledge representation during adaptation, with implications for more efficient fine-tuning strategies and targeted approaches to mitigate catastrophic forgetting.

1 Introduction

In recent years, we have witnessed a rapid proliferation of application of language models (LMs) across virtually every domain. These models demonstrate remarkable capabilities in coding (Nam et al., 2024), mathematical reasoning (Imani et al., 2023), medical diagnosis (Wang et al., 2024), finance (Li et al., 2023), psychological evaluations (Hu et al., 2024), and many more (Lai et al., 2024; Tian et al., 2023; Liu et al., 2024). With the rise in applications, we have models available that vary in size (Kaplan et al., 2020; Touvron et al., 2023), architecture (Gu and Dao, 2023; Dai et al., 2019), context window size (Ding et al., 2023; Chen et al., 2023), and computational efficiency (Dao et al., 2022; Frantar et al., 2023), creating an ecosystem where practitioners have unprecedented options to find the model for their specific application.

Amidst the abundance of these options, finding a balance between accuracy and computational cost that works best for your use case has become challenging. While benchmarking offers a potential solution to this unprecedented problem (Gehrmann et al., 2021; Srivastava et al., 2022), most practitioners prefer to fine-tune base models for their specific niche rather than relying on assistant chat models (Han et al., 2023; Cui et al., 2025; Nguyen et al., 2023). For these base models, perplexity has traditionally served as a performance evaluation metric (Gururangan et al., 2021; Yıldız et al., 2024). However, perplexity suffers from several critical limitations. Most notably, it fails to capture the actual knowledge and focuses mainly on general linguistic model capabilities (Xu et al., 2024; Meister and Cotterell, 2021). Recent research has dived deeper into understanding this issue at token level (Öncel

et al., 2024) and has discovered that lower perplexity scores might stem from domain-unrelated tasks and fail to reflect the actual domain-specific capabilities of the model. These limitations make the perplexity score an unreliable metric for measuring the model capability for a domain-specific task, mainly when focusing on evaluating the domain knowledge.

Benchmarking offers a potential solution as it directly targets domain-specific knowledge rather than measuring the general language capability of the model (Srivastava et al., 2022; Hendrycks et al., 2020), but it also suffers from potential challenges. First, many existing benchmarks for LMs focus predominantly on question-answer formats rather than completion-type formats that would better evaluate base models (Chang et al., 2024; Srivastava et al., 2022; Hendrycks et al., 2020). While studies often use few-shot learning to adapt to this format, model performance in few-shot settings is influenced by factors beyond domain knowledge such as model size (Brown et al., 2020). Additionally, when benchmarks become well established, the data related to these benchmarks (including training sets, test prompts, or even test sets) may inadvertently be included in the pre-training corpora of new models—a phenomenon known as ‘benchmark leakage’ or ‘data contamination’ (Zhou et al., 2023). This issue has become increasingly common as models are trained on ever-larger datasets of public text, and can dramatically inflate evaluation results, creating unfair advantages when comparing different Large Language Models (LLMs) and leading to unreliable assessment of model performance. A potential solution is to employ LLMs to generate benchmarks (Perez et al., 2023; Yuan et al., 2025). This approach has limitations in terms of LLMs’ ability to effectively process and reason over long context lengths (Li et al., 2024), failing to comprehensively ground in the new data without introducing their own parametric knowledge (Monea et al., 2023) especially in large models, and can be computationally expensive depending on the size of input data (Chavan et al., 2024).

To address these challenges, we have developed a deterministic pipeline that converts a raw corpus into a completion-type benchmark without relying on LLMs, ensuring consistent and unbiased assessment across domains. Our approach offers several advantages: (1) it processes raw corpus directly, eliminating data contamination problems present in LLM-generated benchmarks; (2) it can readily incorporate new sources such as recent arXiv papers or domain-specific raw data; (3) it particularly targets base models using completion style prompts while remaining applicable to assistant models; (4) unlike perplexity, it measures the domain knowledge rather than general linguistic capabilities, and more computational efficient as does not require evaluation on each token of a given corpus.

We verified the benchmark created by using our approach through systematic experiments across multiple settings. First, we tested its efficiency on an intuitive task of domain adaptation in the GPT2-XL model. Second, we compared the results against perplexity and the completion task generated by the state-of-the-art model (Claude 3.7 Sonnet) for the same domain. Third, we validated our approach in a continual learning setting with a larger model like Llama to demonstrate scalability. Fourth, we evaluated knowledge acquisition during training by evaluating checkpoints for GPT2-XL and OLMo-2 models. Lastly, we conducted cross-model comparisons to determine the optimal model for specific domain applications.

Beyond benchmarking, we extended our analysis to study how knowledge representation evolves during adaptive pre-training. Previous studies have investigated where factual knowledge is stored in LLMs (Meng et al., 2022; Geva et al., 2020) and how subject-related attributes are encoded across model layers (nostalgebraist, 2020; Dar et al., 2022; Geva et al., 2023). These studies have shed light on the inhomogeneous distribution of factual associations in transformer layers, with mid-layer feed-forward modules playing a crucial role in storing factual associations. While early MLP sublayers contribute to subject representation enrichment and upper multi-head self-attention (MHSA), sublayers perform attribute extraction (Geva et al., 2023). However, little work has been done to understand the knowledge attributes rate analysis combined with domain-adaptive training to trace the evolution of knowledge representation in LLMs during the adaptation process. To address this gap, we developed a mechanistic analysis framework that builds upon our pipeline to investigate the internal changes occurring during adaptation in LLMs. Unlike traditional methods for domain adaptation, which focus on metrics like perplexity (Yildiz et al., 2024; Qin et al., 2022) and benchmark scores (Siriwardhana et al., 2024; Xie et al., 2024), which treat these models as black boxes, our approach reflects the layerwise transformations during domain adaptation.

Building on Geva et al. (2023) approach, we extend our analysis utilizing our pipeline to bridge this gap while employing GPT models to ensure fair comparison to previous works. First, we studied layerwise attribute rate change during domain-adaptive pre-training scenarios. Second, we expanded

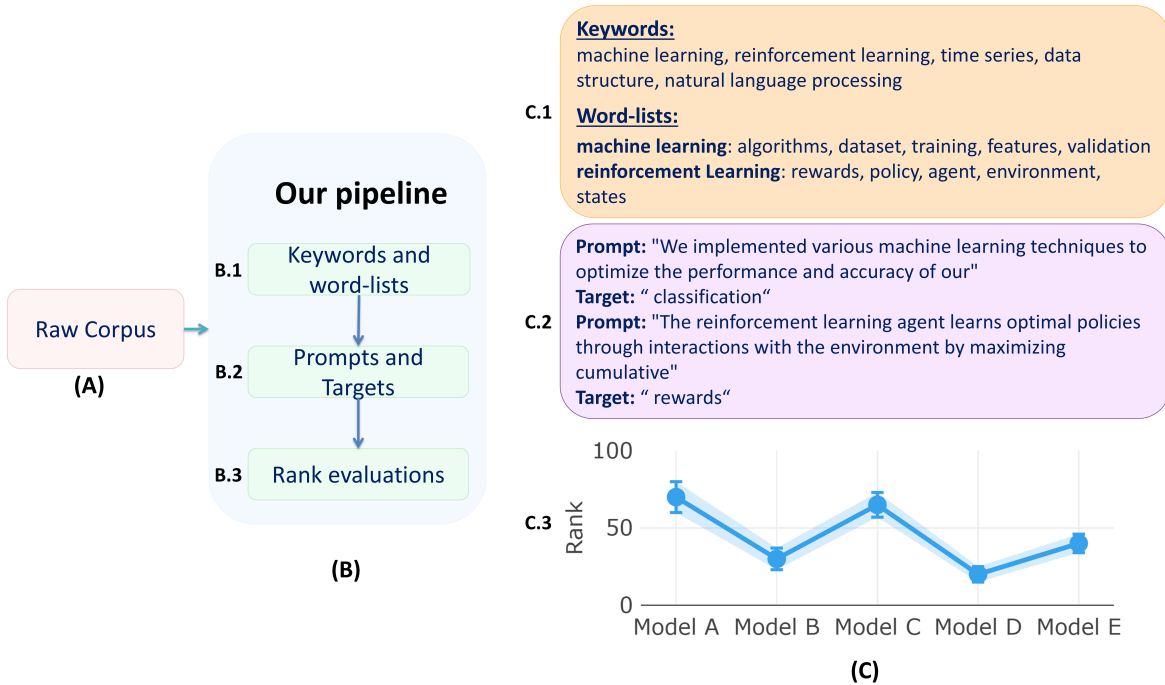


Figure 1: Our proposed pipeline generates a completion-based benchmark given raw data from a domain. It first generates keywords and word lists (B.1/C.1) from raw data. The next step utilizes this output to create prompts and targets (B.2/C.2), where the targets belong to a word list, representing domain-specific words. These prompts and targets are then used as input to the model of interest, and the output (B.3/C.3) ranks (\downarrow) to allow model comparison for a specific task

previous work beyond attribute rate to analyze probability distributions and the percentage change in both metrics, providing a more nuanced view of how these changes are reflected. Lastly, we studied the layerwise evolution of "true" target predictions during adaptive pre-training. These extensions provide a nuanced view into how models acquire and represent domain-specific knowledge, with potential applications for more targeted and efficient fine-tuning approaches. Our findings uncover several key insights:

- i) Our deterministic benchmark evaluation strongly correlates with expert-generated benchmarks while avoiding contamination issues, making it a better alternative to perplexity for measuring domain knowledge.
- ii) Domain adaptation happens rapidly in smaller models (within 500 steps), suggesting extensive training is often unnecessary for domain specialization in smaller models.
- iii) Knowledge acquisition during training follows a pattern of steep initial improvement followed by gradual saturation, enabling potential early-stopping strategies that could significantly reduce computational costs.
- iv) Initial-to-mid layers are primarily responsible for attribute extraction for the input, while the later layer focuses on the next token prediction.
- v) In domain adaptation, forgetting begins in the middle layers where attribute extraction happens, and later layers amplify this effect, revealing how domain knowledge is lost through the model architecture.

2 Methods

This section presents an overview of the dataset preprocessing and describes the intermediate steps to develop our benchmark and evaluation pipeline. The overall pipeline is described in the Figure 1.

2.1 Keyword Creation Pipeline

We implemented a keyword creation pipeline to extract domain-specific n-gram keywords from the arXiv data of the corresponding domain obtained from [Kaggle](#). It consists of abstracts of papers representing document summaries. The pipeline consists of several key stages: data preprocessing, n-gram generation, adaptive threshold-based keyword selection, and similarity-based refinement. In the initial preprocessing stage, we perform text normalization, such as converting text to lowercase, removing bracketed content, handling apostrophes and contractions, and implementing custom tokenization to ensure consistency. Our custom tokenization preserves hyphenated words while separating other punctuation and symbols to maintain the integrity of technical terms.

The next step of the n-gram generation process utilizes the Gensim Phrases model to iteratively build n-grams from size 2 to 7. The algorithm identifies basic bigrams and progressively builds larger n-grams by combining previously identified phrases. For simplicity, we have employed default parameters for a minimum count threshold of 5 occurrences and a collocation threshold of 10 to identify meaningful word combinations.

To ensure the quality and relevance of keywords, the n-grams obtained from the above step then go through a validation process of multiple filtering criteria:

- Regular expression pattern matching to ensure words contain only alphabetic characters and hyphens (e.g., "deep-learning" is valid, "model2" is not)
- Lemmatization followed by filtering against:
 - Stopwords (e.g., "the", "is", "are", "was").
 - Generic academic vocabulary (e.g., "paper", "method", "framework").
 - Function words (e.g., "between", "through", "despite").
 - Quantitative expressions (e.g., "more", "less", "significant").

The third stage implements an adaptive thresholding to select only the most informative keywords. It allows us to determine the proportion of each n-gram to keep in our keyword list. For our work, we have selected proportions of 50% bigrams, 30% trigrams, 15% four-grams, and 5% five-or-more-grams based on empirical analyses. If a domain had n-grams below the given proportion, then the ratios are adaptively adjusted based on the actual proportion of each n-gram length in the corpus. For our corpus, we targeted approximately 300 keywords from each domain.

The final stage is the semantic redundancy reduction based on the similarity score between keywords. We computed the cosine similarity between all keyword pairs using the 'all-MiniLM-L6-v2' model from the Sentence Transformer library and removed the potential duplicates exceeding the similarity score of 0.85. To determine which keyword to keep in case of high similarity between multiple keywords, we applied a hierarchical decision process: first preserving the phrase with shorter string length (e.g., "complex network" over "complex networks"), then for equal-length phrases, keeping the one with higher average similarity to other related phrases. An example of keywords from the Computer Science-Artificial intelligence (CS.AI) domain is presented in Supplementary Table 1.

2.2 Document Preprocessing and Sentence Retrieval Pipeline

2.2.1 Dataset Description

For adaptive training of our models, we have employed the M2D2 dataset [Reid et al. \(2022\)](#). This comprehensive dataset was curated to investigate domain adaptation capabilities in language models. The overall data contains 8.5 billion tokens across 236 distinct domains. It consists of content from both Wikipedia and the S2ORC (Semantic Scholar Open Research Corpus) compiled by [Lo et al. \(2019\)](#). For training, we employed similar parameters as described in [Yildiz et al. \(2024\)](#), i.e., using Adam optimizer with batch size 16 on A100 GPUs, managed via DeepSpeed with 0.2 dropout and automatic learning rate selection.

For any other analysis than training, we have primarily used the arXiv subset of the RedPajama-Data-1T [Computer \(2023\)](#), which contains the full text of 1.56 million arXiv papers and a token count of 28 billion. It is a comprehensive collection of scientific papers from arXiv, a widely used repository of scholarly articles spanning multiple STEM disciplines. This dataset was accessed through the Hugging

Face library, consisting of preprocessed LaTeX source files with removed preambles, comments, macros, and bibliographies. To supplement the full-text from RedPajama-Data-1T, we linked these documents to the arXiv Dataset available on [Kaggle](#) because it provides complete metadata of 1.7 million papers, including title, authors, categories, submission date, abstract, and DOI information.

We combined these two complementary data sources to create a rich dataset with both full-text content and detailed metadata. We mapped these two datasets using arXiv IDs as the linking key. This process successfully matched 1,558,305 documents (virtually 100% of the RedPajama arXiv subset). An example document format presenting both from Kaggle and RedPajama is presented in Appendix [A.1](#).

2.2.2 Data Processing and Sentence Extraction

We employed the above mappings to form a complete text for corresponding research papers by first combining the paper title and abstract from the Kaggle dataset with a colon separator ("title : abstract") and then merging them further with the RedPajama full text. After stripping documents of excess whitespace and empty sentences, we then utilize spaCy's English language model ('en_core_web_sm') to convert these documents into individual sentences.

2.2.3 Embedding Generation and Similarity Computation

We convert these sentences into embeddings using the 'all-MiniLM-L6-v2' model from the Sentence Transformer library. We repeated the same for keywords obtained from Section [2.1](#). Then, we calculated the cosine similarity between the sentence embeddings and keyword embeddings from a given domain to enable the retrieval of sentences based on their similarity to specific phrases.

2.2.4 Sentence Selection and Preprocessing

In the final stage, for each keyword, we set a similarity threshold of 0.5 between the keyword and the corresponding sentence to extract only the sentences semantically related to that keyword. These sentences further undergo a systematic cleaning process. First, any LaTeX-specific formatting was converted to plain text using the LatexNodes2Text library, with error handling to preserve the original text if conversion fails. We removed all citations using expression patterns targeting common citation commands (e.g., `\citet`, `\citep`, `\citett`). We further performed whitespace normalization (converting tabs, newlines, carriage returns, form feeds, and vertical tabs to single spaces), character validation against a predefined set of allowed characters (ASCII letters, digits, whitespace, and punctuation) to remove special characters, and final whitespace stripping. We removed any sentence that failed the character validation from further analyses. In the end, we obtain a clean mapping of sentences for each keyword in a domain of interest.

2.3 Token List: Token Analysis Framework

The token analysis framework follows to get the most relevant tokens for a given keyword. We start by aggregating clean sentences for a given keyword obtained in Section [2.2.4](#) to create a unified document per keyword. We tokenize these sentences using a corresponding model tokenizer we employed in further analysis in Section [2.8](#), and remove all tokens associated with stopwords (NLTK stopwords) or have a character length of less than or equal to 2 characters. We maintain a frequency counter for these filtered tokens. In the final output, we preserve the top 5000 most frequent tokens for each keyword.

2.4 TF Word-List Creation: Preprocessing for Term Frequency Analysis

We developed a term frequency analysis pipeline to extract domain-specific terminology from text corpora. It is a multi-stage process consisting of data aggregation, frequency-based extraction, multi-level filtering, adaptive thresholding, and similarity-based refinement. Again, we combine clean sentences for a given keyword to create a unified document per keyword. For frequency calculation, we employed CountVectorizer from scikit-learn library ([Pedregosa et al., 2011](#)) with a custom token pattern (`r'\s*\w+\b'`) that preserves leading spaces for proper term identification and document frequency thresholds (`min_df=0.00`, `max_df=0.80`) to exclude only the overly common terms across the corpus.

This vectorization process generates the initial term-document matrix capturing raw frequency counts for obtained terms for all keywords.

To ensure the quality and relevance of these terms, the generated frequency counts undergo a multi-level filtering process, including eliminating zero counts and removing stopwords and lower than three-character words. We also removed any term that was not only alphanumeric and only kept the terms that begin with exactly one space so they can later be used as targets in Section 2.6.

To ensure proper terminology extraction regardless of the varying frequency distributions across different keywords, we applied an adaptive threshold to exclude terms that have a frequency score of less than the mean frequency score for each keyword. In the final refinement stage, we applied a similarity threshold of 0.3 between keywords and terms to retain only semantically related terms for a given keyword. For this, again, we employed the same model as mentioned in Section 2.1 for creating sentence embedding ('all-MiniLM-L6-v2') for both keywords and obtained terms. Supplementary Table 1 column "Word-list (TF)" presents 10 examples of word-list obtained from this method for given keywords from the CS.AI domain.

2.5 TF-IDF Word-List Creation: Preprocessing for Term Frequency-Inverse Document Frequency Analysis

Our TF-IDF (Term Frequency-Inverse Document Frequency) analysis pipeline is similar to the term frequency analysis as discussed in the above section as it also consists of a multi-stage process following similar steps, such as data aggregation, TF-IDF based extraction, multi-level filtering, adaptive thresholding, and similarity-based refinement. The critical part that differs is the calculation for TF-IDF based extraction instead of frequency-based extraction, and we use adaptive thresholding on the TF-IDF score for mean thresholding instead of the counter value of corresponding terms.

For TF-IDF based extraction, we employed TfidfVectorizer from scikit-learn with a custom token pattern (`r'\s*\w+\b'`) that preserves leading spaces for proper term identification and document frequency thresholds (`min_df=0.00, max_df=0.50`) to exclude only the overly common terms across the corpus. The reason for the strict threshold for `max_df` is to encourage only the niche terms related to the keyword by penalizing the repeated terms across keywords more strongly. Supplementary Table 1 column "Word-list (TF-IDF)" presents 10 examples of word-list obtained from this method for given keywords from the CS.AI domain.

2.6 Prompt-Target Pair Construction

Our prompt-target pair construction pipeline utilizes keywords (Section 2.1), their word lists (TF and TF-IDF, corresponding to Section 2.4 and 2.5 respectively) and the cleaned sentences (Section 2.2.4) to generate prompts and targets for a domain of interest. The pipeline consists of prompt filtering, two-pass term matching, prompt-target extraction, and balanced sampling across domain vocabulary.

In the first step, we retrieve the cleaned sentences for keywords described in Section 2.2.4 using a similarity threshold of 0.5. Then, we filter out these further by conditioning a minimum context length of 10 tokens and 40 characters. It ensures enough context for language models to predict the corresponding target. The later part of filtering is removing all the sentences with no matching term from the word list after the 10th token. Selecting a target involves a matching algorithm to identify precise positions where domain terms occur. It consists of two passes for term matching from the word list as follows:

1. **First pass:** We scan the tokenized sentence starting from a position slightly before our minimum context length (token length of 6). At each position, we check if the subsequent tokens match any domain-specific term in our word list for a given keyword. If the matches are found, we record both the starting and the ending positions.
2. **Second pass:** We filter the matches to retain only those that:
 - Start at or after our minimum context length
 - Have no other term from the word list ending immediately before them to prevent overlapping.

If multiple valid matches exist in a sentence, we randomly select one to ensure diversity in our evaluation data. In the end, we have a prompt that makes up all tokens up to (but not including) the match position of the term from the word list, and the target is the matched domain-specific term from the word list. This process is repeated for each keyword of the corpus until the desired number of prompts are created or there are no more clean sentences left for that keyword. These prompts and targets are created separately for TF and TF-IDF word lists and thus are evaluated separately because of the different difficulty levels. Supplementary Table 2 presents an example of our prompt creation pipeline from the arXiv dataset from two domains. For each keyword, 50 prompts and targets were created for both TF and TF-IDF cases to represent the diversity of the domain.

2.7 Model Evaluation Pipeline

Utilizing prompt-target pairs, we evaluate each model’s ability to predict the target given only the preceding context using the ranks and probability for the target token. We first tokenize the prompts and target tokens by the model’s native tokenization scheme before evaluation. We took our smallest model (GPT-2 XL) and removed any prompt-target pairs that exceeded the model’s context window limitation to ensure a fair comparison. If the target consists of multiple tokens, then after the prediction of the first target token, the subsequent prompt is created by including the true first target token with the prompt to predict the next target token, and the rank and probability for this prompt were averaged over all the predicted ranks and probabilities of the target tokens. In the result section, we report mean and median ranks along with Confidence Interval (CI) and probabilities over all the prompts from all the keywords for that domain.

2.8 Attribute Rate Calculation

We adopted and extended the attributes rate analysis introduced by Geva et al. (2023) to understand knowledge progression through layers in LLMs. This metric helps quantify the subject-related information contained in each layer’s representations. In our work, subjects refer to the keywords we extracted in Section 2.1.

2.8.1 Methodology

For a given keyword, the attributes rate computation involves two components: The first component represented by top- k are the top k clean tokens obtained by projecting the hidden activations h_i^ℓ at position i and layer ℓ to vocabulary space after removing the stopword-related tokens and tokens with characters fewer than 3. The second component is the cleaned tokens for each keyword calculated in Section 2.3 represented by A_s . Similar to Geva et al. (2023), we calculate attribute rate for a given keyword as

$$\text{Attribute Rate} = \frac{|\text{Top-}k \text{ tokens} \cap A_s|}{k} \times 100\% \quad (1)$$

And the projection for tokens from LLM is calculated as

$$\text{projs} = h_i^\ell \cdot E^T \quad (2)$$

where E is the model’s input embedding matrix. In our analysis, we mainly focus on the last token of the keyword as it can attend to all preceding subject tokens and thus contains the most comprehensive subject representation, as demonstrated by the attributes rate analysis Geva et al. (2023).

We have extended the original implementation from Geva et al. (2023) to add layer normalization before hidden activation projection to vocabulary space. The original analysis only focused on the rank, i.e., top- k tokens from LLM, whereas our analysis also focused on probability for these tokens that are part of the attribution rate for each layer. We calculated the layer norm

$$h_{\text{normalized}} = \text{LayerNorm}(h_i^\ell) = \frac{h_i^\ell - \mu}{\sqrt{\sigma^2 + \epsilon}} \cdot \gamma + \beta \quad (3)$$

Where μ and σ^2 are the mean and variance of the hidden state, ϵ is a small numerical stability constant from the model’s final layer normalization, and γ and β are the trained scale and shift

parameters from the model’s final layer normalization applied during inference. So, the modified projection in our case is given as:

$$\text{projs} = \text{LayerNorm}(h_i^\ell) \cdot E^T \tag{4}$$

Without normalization, we observed that probability distributions towards the final layers exhibited abrupt changes that did not align with the model’s actual output probabilities. Layer normalization helps capture the smooth progression of probabilities across layers and ensures the projected probabilities in the final layer match the model’s output, providing a more accurate view of how information flows through the network.

In addition to the attributes rate, we calculate the sum of probabilities metric. We define it as follows:

$$\text{Probability Sum} = \sum_{t \in \text{Top-}k \text{ tokens} \cap A_s} P(t) \tag{5}$$

where $P(t)$ represents the probability assigned to token t when projecting the subject representation to the vocabulary space. This metric provides a complementary measure of how strongly the model associates the keyword with relevant attributes, as it accounts for the probability mass assigned to overlapping tokens rather than just their presence in the top- k set.

2.9 Last Layer Attribute Rate for Cross-Architectural Comparison

While the layerwise attributes rate provides a deep insight into the progression of enrichment of the subject as it passes through each layer in LLM. This method has mainly been employed for GPT family models (nostalgebraist, 2020; Dar et al., 2022; Geva et al., 2023) and does not work well for models such as Llama-2, Llama-3.1, and OLMo-2 with other models because of architectural differences, making direct projection of hidden states potentially incomparable across architectures. To address this limitation, we implement a cross-architectural comparison focusing exclusively on the final layer representations since the last layer’s hidden state projection corresponds to the model’s token prediction and their corresponding probabilities, which can be easily accessed for each model by default. It is particularly relevant as the attribute rate typically follows a monotonic increasing pattern through the layers as shown in Geva et al. (2023), with the final layer representing the culmination of the subject’s enrichment throughout the model.

2.10 Benchmark Creation Using Claude

To test the validity of our method, we wanted to test it against a benchmark. We tried to find a benchmark suitable for base models, which consists of completion tasks for measuring knowledge because small models like GPT-2 medium/XL and Llama-2 7B employed in our study as they are sensitive to formatting of questions and do not follow well on few shot learning tasks as shown in Brown et al. (2020) and we also demonstrate an example in Section A.2. Given that our task is a completion task for base models, we also wanted to compare it against the completion benchmark to quantify the model’s knowledge of the domain of interest. Because of the unavailability of a benchmark that satisfies our criteria, we used state-of-the-art models from Anthropic (2025), i.e., Claude 3.7 Sonnet, to create a benchmark for our domain of interest. First, we asked Claude to generate 20 keywords from a given domain after giving an example of our extracted keywords from the corresponding domain. Then, we asked it to generate 50 prompts for each keyword and their corresponding targets by providing a few examples. For the CS.AI domain, the keywords generated by Claude include Neural Networks, Reinforcement Learning, Natural Language Processing, Computer Vision, etc. The table below presents two examples of the first three keywords generated by Claude.

Neural Networks:

Prompt: The basic computational unit in neural networks is called

Target: neuron

Prompt: The specialized neural network designed for image processing is called

Target: convolutional neural network

Reinforcement Learning:

Prompt: The entity that takes actions in reinforcement learning is called

Target: agent **Prompt:** The algorithm that combines Q-learning with deep networks is called

Target: DQN

Natural Language Processing:

Prompt: The task of determining word classes in a sentence is called

Target: part-of-speech tagging

Prompt: The model architecture that revolutionized NLP with attention is called

Target: transformer

2.11 Perplexity Calculation

For perplexity calculation, we employed the test set from the M2D2 domain to avoid data leakage problems. The reason we are using the M2D2 test set and not the arXiv dataset is because the arXiv dataset is formatted in latex, resulting in high perplexity and does not give a fair estimate of model performance. M2D2 test data, on the other hand, is cleaned raw text data widely used for perplexity measure (Yildiz et al., 2024; Öncel et al., 2024).

3 Results and Discussions

3.1 Part 1(a): Domain Adaptation Within the Same Model

This section describes the experiments that compare one model type. This means the base model is fixed, and we are comparing domain adaptation and checkpoints during training and adaptation on the base model for different cases as described below:

3.1.1 Domain Adaptation of GPT2-XL Models

This task aims to follow an intuitive order to validate our benchmark. We trained the GPT-2 XL base model on the M2D2 train dataset from computer science-related domains (Artificial Intelligence (AI), and Computation and Language (CL)), domains unrelated to computer science (Culture and Humanities, and Material Science), and adaptive pre-training the unrelated domains on CS.AI (CS.AI + Material Science and CS.AI + Culture and Humanities). In total, we have six adapted domain models and one base GPT2-XL model. We tested these domains on the benchmark created by Claude that acts as a "True" benchmark and our prompt-target creation method from TF and TF-IDF based targets from the arXiv dataset from the CS.AI domain. We further tested this model's last layer attribution rate using the tokens obtained from the arXiv CS.AI domain and perplexity measure from the M2D2 CS.AI domain test dataset.

We can see an expected trend in Figure 2 for the result of this analysis. For the "True" benchmark made using Claude, computer science-related domains perform the best; the second best-performing domains are those adaptive to the computer science domain; then comes the base model; and lastly, the ones trained on unrelated domains. This task was kept simple to test the reliability of the "True" Claude benchmark and compare it against our benchmark creation. As we can see, the results follow the intuitive order for ranks increasing from left to right, and our introduced pipeline shows a significant correlation with the Claude benchmark as shown in the left of Figure 3. We further examined the validation of these results by comparing the top and bottom 25% targets' cosine similarity by employing a sentence transformer to get embeddings for these targets with the phrase "Computer Science Artificial

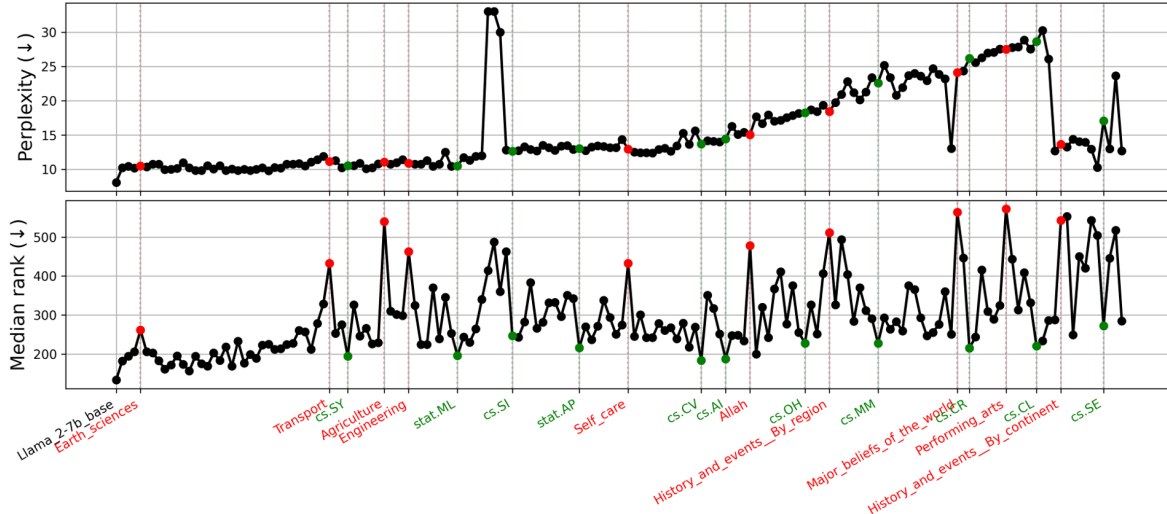


Figure 4: The above figure shows continuously trained Llama-2 models on the M2D2 dataset tested on the CS.AI (arXiv) domain. We can observe a pattern, i.e., minima for domains in M2D2 related to CS.AI (green) and maxima for completely unrelated domains (red) for our TF rank analysis method. On the other hand, perplexity does not show any such pattern, making it unreliable for measuring domain knowledge.

Intelligence” for cases where the CS.AI domain adapted model performed better than the base model. We can see the results in the right side of Figure 3, which show a significant difference between these top and bottom 25% target terms, confirming that the targets where CS.AI adapted domain model performed significantly better are indeed relevant to the CS.AI domain. Although the difference is significant, we still do not see much difference between the left and right violin plots because the targets were created to be relevant to CS.AI. Hence, even the bottom targets show good cosine similarity values. The details of this method are described in Supplementary Section A.3, and the figures for mean metric ranks are in Supplementary Figures 13 and 14.

3.1.2 Continual Learning in Llama Model

We conducted a continual learning experiment on the Llama-2 model, continually trained on 165 M2D2 domains as described in Yıldız et al. (2024). We tested it on the CS.AI arXiv dataset for TF ranks and the CS.AI test dataset of the M2D2 for perplexity. We found that the minima in ranks (lower the better) appear for the domains related to CS.AI, shown by green dots in Figure 4, and maxima are for unrelated domains, shown by red dots. This is expected behavior as the model, when trained on CS.AI-related domains, evidently performs better compared to the model trained on unrelated domains, displaying the reliability of our introduced benchmark and rank method. However, perplexity does not seem to follow any such pattern and hence does not yield any information about the actual domain knowledge.

3.1.3 Checkpoint Evolution During GPT2-XL Adaptive Pre-training

We compared our introduced benchmark and evaluation method for tracking the effects of domain adaptation for the GPT-2 XL model during training. We call the GPT-2 XL model the base model, whose metrics are considered as the baseline as shown by the black dotted horizontal line in Figure 5, and the CS.AI final (red dotted line) represents the value of metrics corresponding to the final checkpoint on the model adapted to the CS.AI domain from the M2D2 dataset. Each model starts from either the base model or from a pre-adapted model and is trained on equal steps of data for fair comparison from the target domain of interest because each domain has different amounts of data available in the M2D2 dataset, and each step corresponds to a batch size of 16. The start and end domain is mentioned in the figure legend. For example, ”CS.AI to Materials” means the starting model was an adapted model on the CS.AI domain and is further trained in steps on data from the Materials Science

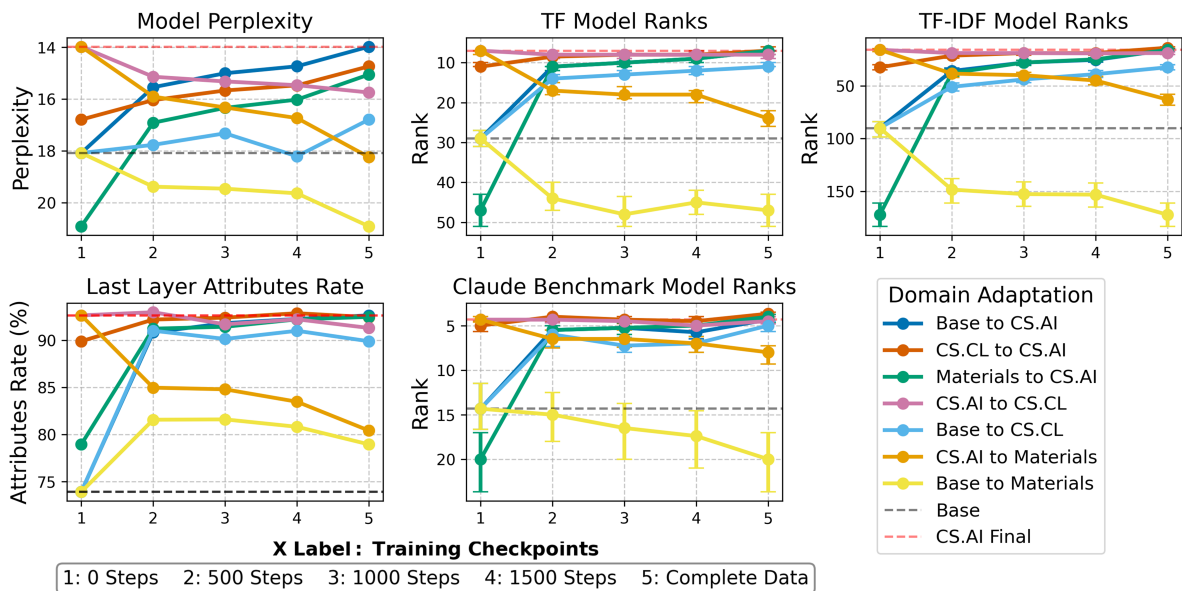


Figure 5: The figure shows the evolution of different metrics for the GPT-2 XL model while being adapted to different domains. Each step corresponds to an equal amount of data trained on the target domain for fair comparison. We can see the heavy dependence on the ending domain and some influence on the starting domain. For smaller models like GPT-2 XL, we can observe that even a small amount of data results in significant adaptation to the new domain knowledge.

domain. The results presented for the test conducted for these metrics on the CS.AI dataset from arXiv except for perplexity as mentioned in Section 2.11, which was performed on the test dataset from the M2D2 domain.

We can see a consistent pattern, as expected, in all of the metrics. The domain with CS.AI as the target domain performs better than other adapted models, showing the dominance of the target domain over the initial domain. CS.CL (Computer Science - Computation and Language), as expected because of its proximity to the CS.AI domain, turns out to be the second-best performer. Models whose target ends at Materials Science seem to perform worst out of all because of irrelevance to the CS.AI domain. When the target is fixed, we can see a similar pattern for the initial domain as well; for example, out of the models that have Materials Science as the target domain, the model started from the base GPT2-XL model has far worse rank, perplexity, and attribute rates than the one started from the CS.AI domain.

We can also observe that for smaller models like GPT2-XL, the domain adaptation happens very rapidly, even with a small amount of data, as can be seen by a strong jump in each metric for 500 steps of adaptive training. This implies that for smaller models, we can achieve significant improvement without the need to spend a high computational budget for domain adaptive training.

TF and TF-IDF model ranks seem to perform very similarly to the Claude benchmark. Perplexity, although on average displaying a similar trend, shows somewhat peculiar behavior for "CS.AI to Materials" and "Base to CS.CL" cases. We expect that the model that has been trained on a related domain should perform better than one trained on an irrelevant domain, which seems to be the case with all other metrics, demonstrating the limitations of perplexity compared to our robust method of rank evaluation from our introduced pipeline.

3.1.4 OLMo-2 Checkpoint Evolution During Model Training

To evaluate the effectiveness of our method in measuring domain knowledge acquisition during training, we analyzed TF model ranks for OLMo-2 checkpoints under two scenarios: 1) the first 50 checkpoints and 2) equally spaced checkpoints throughout training. Figure 6 demonstrates the expected pattern of decreasing TF rank for the Physics and Society domain. The left panel displays the first 50 checkpoints, with the rightmost point on the x-axis corresponding to the fully trained base model. We observe a steep decline in model ranks during initial training, which is expected as the weights evolve from their

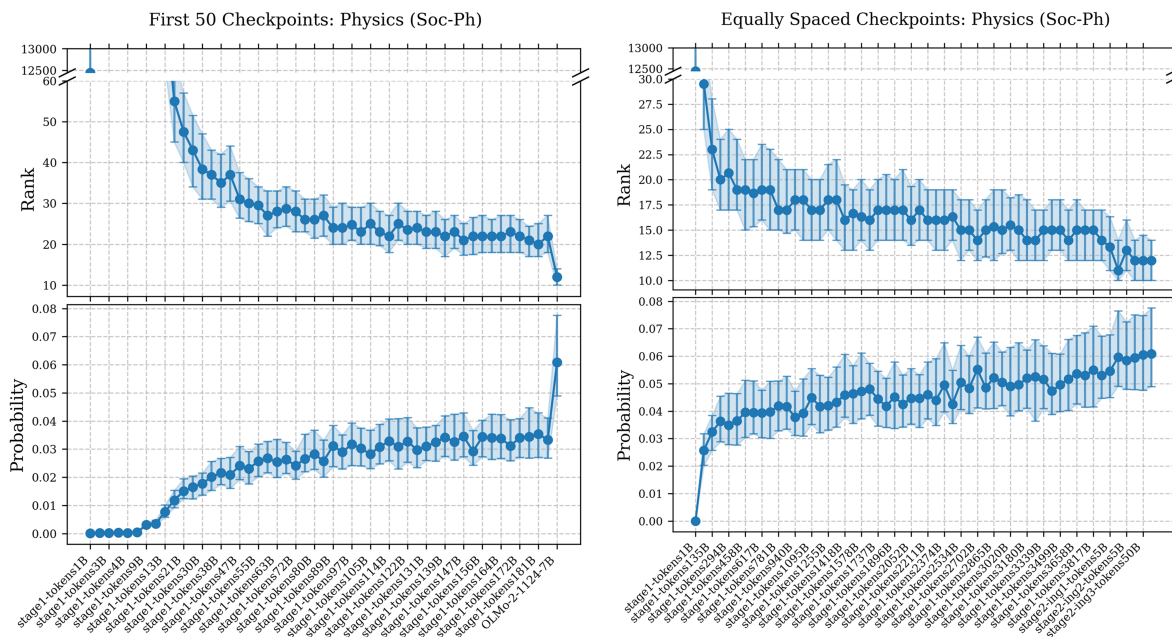


Figure 6: The figure shows the evolution of TF median rank and probability for OLMo-2 checkpoints on the Physics and Society domain from the arXiv dataset. The left figure displays the evolution of rank across the first 50 checkpoints, with the last data point representing the base model for reference. The right figure corresponds to 50 equally spaced checkpoints from stages 1 and 2, plus 6 checkpoints from each ingredient step, totaling 56 checkpoints, with the base model included at the end for reference. This demonstrates the potential of our approach to better guide the training process for a domain of interest by replacing perplexity with metrics more directly related to domain knowledge.

random initialization state and align during the training process. This rapid decline continues for approximately 25% of the initial checkpoints before the rate of change diminishes. Notably, even at the 50th checkpoint, a significant difference in rank persists between this intermediate state and the final base model, indicating substantial potential for further training in this domain.

For the second analysis, we selected 50 equally spaced checkpoints from stage 1 (out of 928 total checkpoints). From stage 2, which consists of three ingredients with 12 checkpoints each, we selected the first and last checkpoints from each ingredient, resulting in 56 checkpoints for this analysis. In instances where checkpoints were corrupted, we substituted the next available checkpoint. A comprehensive list of all evaluated checkpoints is provided in Supplementary Table 4. The right panel of Figure 6 illustrates that while the downward trend continues through later training, the differences between subsequent ranks are substantially minor compared to the first 50 checkpoints, suggesting a gradual saturation from extensive training. The final data point, representing the base model, shows a minimal difference from its preceding checkpoint, reflecting the negligible difference in training tokens between these two models. The probability plots also provide a better alternative to look at the rank change because it is constrained between 0 and 1, making it easy to interpret significant rank changes directly, as in the checkpoint evaluations.

We also conducted an evaluation for the CS.AI domain, depicted in Figure 15, which exhibits a similar trend with one notable distinction: the overall ranks are considerably lower compared to the Physics and Society domain, indicating the relative ease of the CS.AI task for the model, perhaps because of relatively abundant data in training from this domain, resulting in earlier saturation of performance. A significant advantage of our methodology is its potential to reduce computational costs by identifying early domain-specific saturation. Furthermore, given its reliability compared to perplexity scores, our approach could potentially replace perplexity metrics when developing domain-specialized models.

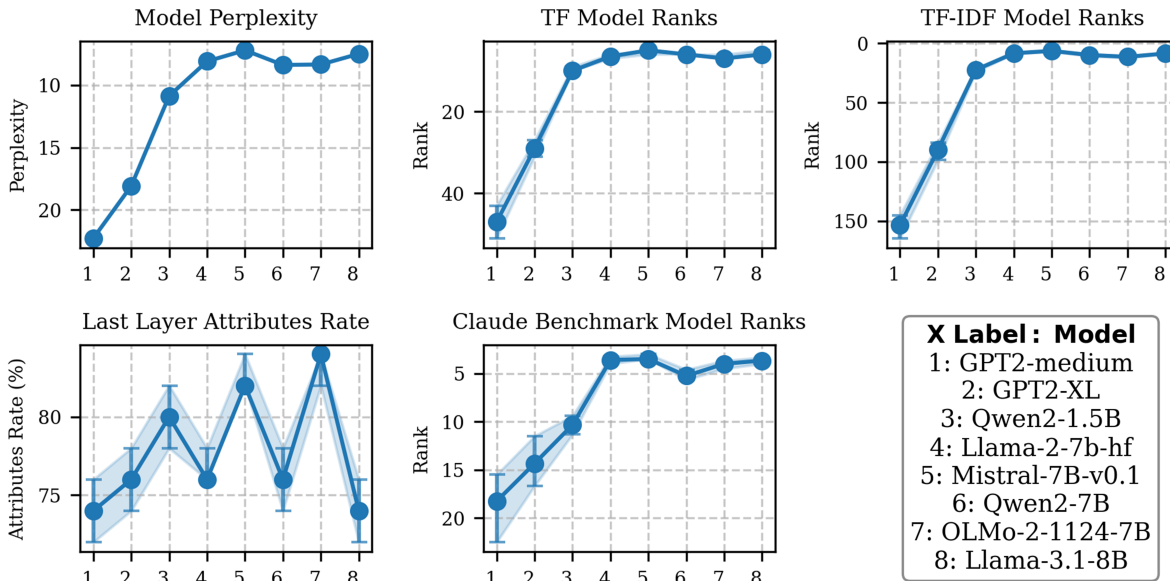


Figure 7: It illustrates the median ranks, attribute rates, and perplexity values for eight distinct models evaluated on the CS.AI dataset. We observed a high correlation between our introduced benchmark metrics (TF and TF-IDF ranks) with perplexity and the "True" benchmark generated by Claude.

3.2 Part 1(b): Domain Adaptation Between Different Model Types

This section will describe the experiment that compares models of different families. This means we are comparing models with different architectures, parameters, and sizes.

3.2.1 Comparison Across Eight Models of Different Sizes

To identify suitable models for specific use cases, we conducted experiments on eight models of different architectures and sizes to compare knowledge for the CS.AI domain, and the results are shown in Figure 7. As a reminder, the TF and TF-IDF ranks and last layer attributes rate shown were calculated on the arXiv dataset from the corresponding domain, Claude benchmark model ranks were calculated on the Claude generated benchmark, and perplexity on the corresponding domain’s test dataset from the M2D2 dataset. We can observe that our proposed method (TF and TF-IDF ranks) seems to closely follow the Claude-generated benchmark ranks. We can see a very similar pattern in model perplexity, hence corroborating the validity of our introduced benchmark. Considering the Claude benchmark as a "True" benchmark, we ran the correlation analysis as shown in Figure 8, where the TF and perplexity method both shows significant correlation with the Claude benchmark, but not the last layer attributes rate.

The same pattern can also be seen for the mean ranks as shown in Supplementary Figure 16. We chose the median rank as more reliable than the mean rank because the median is more robust to outliers, given that certain prompts generated by our pipeline might not have all the context to answer the prompt, affecting the overall rank metric calculation. We verified the validity of our results by repeating the same experiments in the Physics and Society domain. The results remain almost similar to they are for the CS.AI domain, as can be seen in Supplementary Figure 18, 19, 20, and 21.

3.3 Part 2: Attribute Rate, Rank, and Probability Analysis During Adaptive Pre-training

We will present the results on the attributes rate from Geva et al. (2023) and our extended work on this approach and analyze it in a domain adaptive setting.

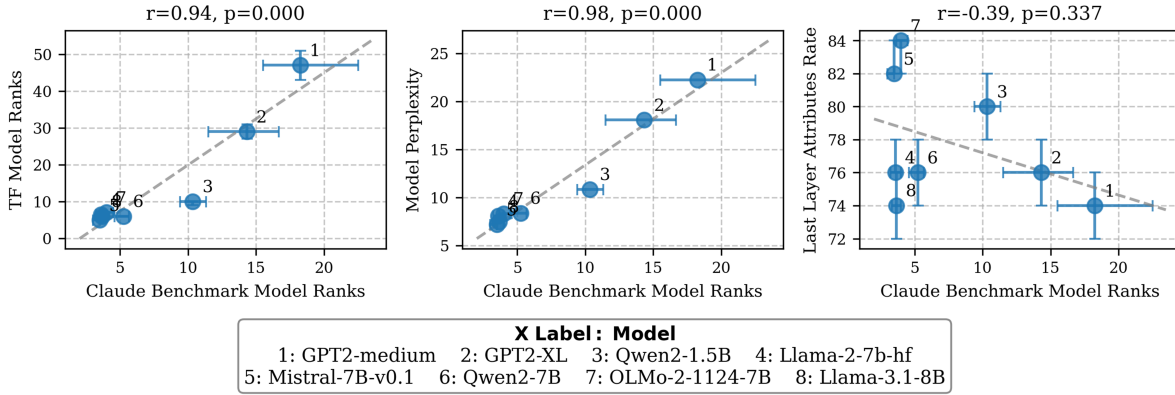


Figure 8: Correlation plot for the Figure 7 shows almost no correlation between the Claude benchmark and the last layer attributes rate. On the other hand, it shows a significant correlation with the TF ranks and perplexity.

3.3.1 Attribute Rate and Extended Analysis

Two essential components describe the overall shape of the attributes rate curve, i.e., the number of clean tokens from each layer output and the number of clean tokens corresponding to each keyword. To be consistent with Geva et al. (2023), we utilized 50 tokens from each layer for a given keyword as input and approximately 1200 tokens for each keyword, and we present different variations of these tokens and their effect on the attributes rate averaged over all keywords in Supplementary Figure 22 for GPT2-XL model tested on CS.AI arXiv dataset created keywords and corresponding tokens. We can notice that the y-axis (attributes rate) is much higher (70-90) as compared to the results presented in Geva et al. (2023). It happens because, in Geva et al. (2023), the analysis involves handling all the tokens found by the BM25 algorithm from Wikipedia pages for a particular keyword obtained after cleaning. It does not exclude tokens that might not be relevant to the subject/keyword. On the other hand, because of the availability of abundant text data for a given keyword, we took only the most frequent tokens for a given keyword, and hence, the relevance of tokens resulted in a high attributes rate, making our approach more domain-focused by removing irrelevant tokens. We extended the original approach to include a layer norm component, as seen in Figure 9. We can notice on the left panel that without layer norm, the model probability shows a sudden drop in the probability for the last layers. This abrupt change happens because the logits in the later layers exceed the previous layers significantly, and the probability also behaves similarly. When the layer norm is applied to each layer, the changes become much more smooth and interpretable, and no abrupt changes happen towards later layers. We refer to Figure 10 to understand the dip in the sum of probability plot towards the last layers of the LLM. The dashed line in the figure represents the average sum of probabilities over all keywords for the 1200 keyword tokens found in the top 50 clean tokens for each layer prediction for a given keyword. The dotted line represents the sum of probabilities of tokens that lie in the top 50 token predictions from each layer and are not part of the attributes rate tokens. We can observe that the initial till mid layers focus on enhancing the attributes for a given keyword and collect all the related tokens for that keyword. Starting at layer 30, the model starts focusing on predicting the next token. We want to note that as the input to the LLM is a keyword example, "machine learning," the next token prediction will have a high probability of predicting a stopword, for example, "is," "are," or another stopword. Hence, the average likelihood for these tokens increases, and the probability sum of the attribute token starts decreasing. A list of tokens in the top 50 predictions that are in the token list of the keyword (dash line) and not in the token list (dotted line) is given in Supplementary Table 5 for five keywords. To be consistent, if not mentioned otherwise, we will only further investigate the case with layer norm, with 50 clean tokens from LLM prediction and 1200 tokens per keyword and the keywords and corresponding tokens created from the arXiv CS.AI domain dataset.

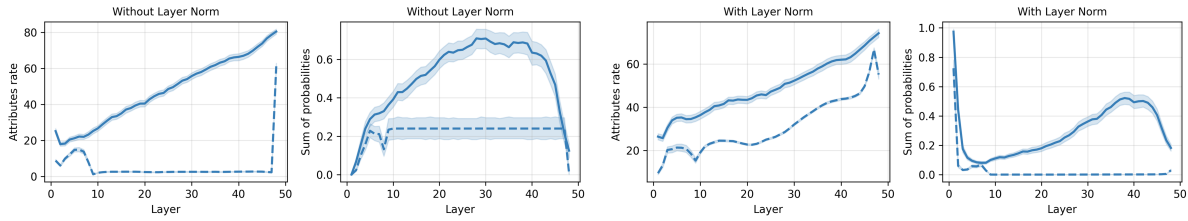


Figure 9: For GPT2-XL model, the left panel shows the method employed by [Geva et al. \(2023\)](#), which does not have component for layer norm. The reason for introducing layer norms is to deal with the abrupt changes in the later layers. As we can see in the above plot of the sum of probabilities on the left panel without layer norm, for the last layers, the decrease in probability is quite drastic because if we look at the logits, they are almost similar for the last few layers and do not match the actual model output. On the other hand, the right panel with layer norm has no drastic changes in the probability for the later layers.

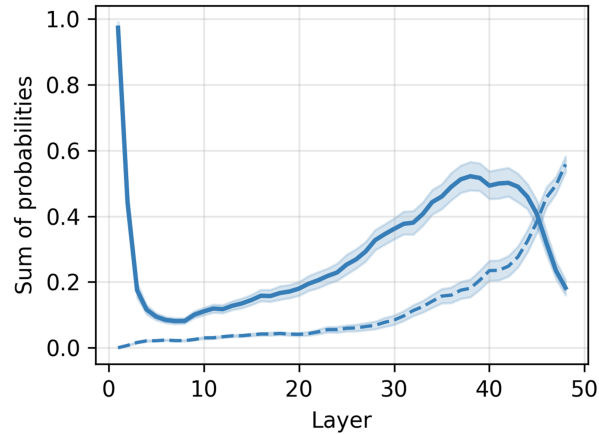


Figure 10: The dashed line is the sum of probabilities for the 1200 tokens for keywords found in the top 50 clean tokens for each layer for the given keyword. The dotted line represents the sum of probabilities of tokens that lie in the top 50 token predictions from each layer and are not part of the attributes rate tokens. We can see that later layers start to build up on the next token prediction, and the probability for keyword-related tokens starts plummeting.

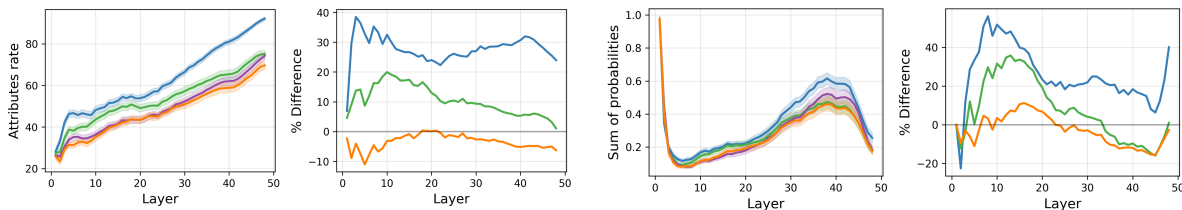


Figure 11: Figure shows the change in the attributes rate, the sum of probability, and percentage changes for both metrics compared to the base model for GPT-2 XL for different domain adaptation settings. The major changes happen in the middle layers where the attribute extraction occurs for the keywords, indicating that knowledge storage and changes are associated with the initial to middle layers.

3.3.2 Attribute Rates and Sum of Probabilities in Domain Adaptive Setting

We experimented with domain adaptive pre-training to see how the attributes rate and sum of probabilities change after adapting to a particular domain. As we tested on keywords and corresponding tokens created using the arXiv CS.AI domain dataset, therefore we tested for the models adapted to domains that were relevant to CS.AI, continually pre-trained from CS.AI to the irrelevant domain (CS.AI + Cultural and Humanities), the base model and base model adapted to irrelevant domain (Cultural and Humanities) from M2D2 dataset. We introduced the percentage difference for attributes rate and the sum of probability metric defined as an increase in the target domain compared to the base, i.e. $(\text{target} - \text{base}) * 100 / \text{base} \%$, to see which layers are most affected by the domain adaptation. From the results in Figure 11, we can see that training on a relevant domain led to an increase in both attribute rate and the sum of probabilities, indicating the increase in domain knowledge. Further training on an unrelated domain (CS.AI+ Culture) takes a minor hit on both metrics because of potential forgetting phenomena (Kirkpatrick et al., 2017). In the percentage difference plots, we can see that the significant changes in both metrics happen around the initial to mid layers, hinting at the finding that these layers are primarily responsible for considerable attribute extraction as also indicated by Meng et al. (2022). As described in Figure 10, the model starts focusing on the next token prediction after the attribute extraction happens, and hence, the attribute rate goes down. However, if we observe the final percentage difference, the CS.AI-adapted domain model still significantly increases the probabilities of the relevant tokens to the keyword, focusing more on domain knowledge than the base model. Comparing the CS.AI domain adapted model and this being further adapted to the Cultural and Humanities domain (CS.AI + Culture), we can see the effect of forgetting happens first significantly in the middle layers where attribute extraction happens and gets worse in the later layer, where next token prediction happens, indicating the later layers amplify this effect carried from earlier layers. A similar analysis was performed for GPT-2 medium adaptive models shown in Supplementary Figure 23, where the relative effects of adaptive training are less pronounced as compared to the GPT2-XL model but follow a similar pattern.

3.3.3 Layerwise Rank and Probability Changes for Prompt-Target Approach in Domain Adaptive Setting

We further tested the adaptive pre-training effect on ranks and probabilities for each layer for the correct target by utilizing our introduced pipeline prompts and targets described in Section 2.6. Because of the high computational cost involved for layerwise prediction, we ran this analysis only for 100 keywords and 30 prompt-target each, resulting in approximately 3000 prompts. We also studied the percentage change in the different adapted domain models for ranks and probabilities, where % change is defined as the $(\text{target} - \text{base}) * 100 / \text{base} \%$ for both metrics, where the target is the adapted domain model. We employed the same models described in Section 3.3.2 because we utilize the CS.AI domain arXiv dataset to create these prompts and targets. For the GPT2-XL model, the results are shown in Figure 12. We can observe that the rank (lower the better) and probability (higher the better) improve when the adapted domain is relevant to the evaluated domain as expected, and minor changes in both metrics were observed for the domain adaptation on an unrelated domain to the target domain. The significant changes happen in the initial to mid layers and later layers for probability but only in the

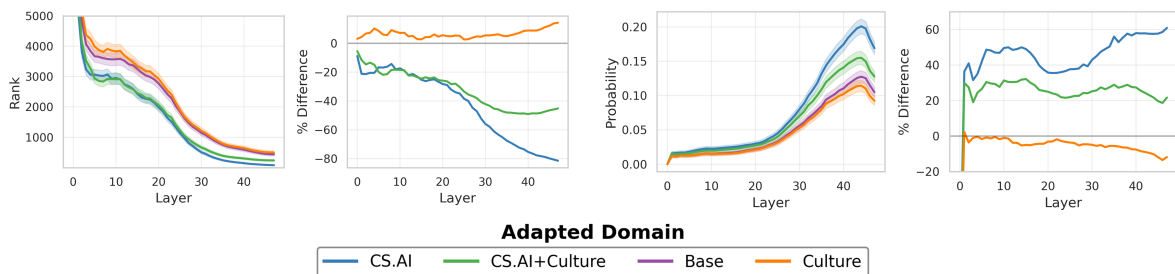


Figure 12: Layerwise rank and probability for tracing the correct target for GPT-2 XL model adapted to different domains on M2D2 dataset. We can see an overall improvement in both metrics because, unlike Section 3.3.2, we trace the actual output. Hence, the later layer percentage probability difference does not go down.

later layers for the ranks. This time, we do not see any dip below zero percentage in the percentage change probability plot because, unlike the analysis on attributes rate, here we are only tracking the probability of the actual target, hence as seen in Figure 10, as the later layers focus on the prediction of the correct token, we can see an overall increase in the probability and rank in the later layers. The results are consistent with our other analyses in this section as we can observe a combined effect of two analyses here, i.e., the enhancement of the token probability in the middle layers and further boost in the later layers because we are tracking the actual target prediction, where Section 3.3.2 explains the bump in the probability in initial to mid layers and Section 3.3.1 explains the further target token enhancement in the later layers. For probabilities, this effect can be seen more clearly than ranks, where the increase in later layers significantly outweighs the enhancement of the middle layers because of the difference in the scaling of these metrics. Here also, we can observe the effect of forgetting while comparing CS.AI with CS.AI+Culture as observed in the previous Section 3.3.2, which is exaggerated in the later layers during the next token prediction. A similar trend can be seen for the GPT2-medium domain adaptation case, as shown in Supplementary Figure 24, illustrating the consistency of our results. Focusing only on the probability plot, we can see that probability goes down slightly for the last layer. We speculate this might be because of the effect described in Sharma et al. (2023), that higher-order components in later layers can encode either incorrect answers of the same semantic type as the correct answer or generic high-frequency words like 'the' or 'of,' which when combined with low-order components produce a sort of 'average answer' that is likely incorrect in some cases, and hence decreasing the overall accuracy of the target prediction.

4 Related Work

4.1 Evolution of Language Model Evaluation

The evaluation in large language models (LLMs) has changed significantly over time, starting with statistical measures like perplexity (Jelinek et al., 1977; Gururangan et al., 2021; Yildiz et al., 2024). Even though widely employed, it fails to capture the actual domain knowledge and focuses primarily on the linguistic capabilities (Xu et al., 2024; Meister and Cotterell, 2021; Öncel et al., 2024). This limitation shifted the evaluation using benchmarking approaches, exemplified by frameworks like GLUE (Wang et al., 2018), SuperGLUE (Wang et al., 2019), MMLU (Hendrycks et al., 2020), BIG-bench (Srivastava et al., 2022), and GEM (Gehrmann et al., 2021), which aim to evaluate the target knowledge and reasoning capabilities directly. However, these benchmarks face challenges, including "benchmark leakage" or "data contamination" (Zhou et al., 2023; Lewis et al., 2020), the prevalence of question-answer formats over completion-type tasks (Chang et al., 2024; Srivastava et al., 2022; Hendrycks et al., 2020), and the dependence of few-shot performance on model size rather than domain knowledge (Brown et al., 2020). Because of the very high human cost associated with developing ever more new benchmarks to deal with the above issues, recent research has explored automated benchmark generation using language models (Perez et al., 2023; Yuan et al., 2025). But this approach struggles with processing long contexts (Li et al., 2024), grounding in new data without introducing parametric knowledge (Monea et al., 2023), and computational efficiency (Chavan et al., 2024). Recently,

LiveBench [White et al. \(2024\)](#) has addressed contamination concerns by incorporating questions from recent external sources with objective ground-truth scoring without relying on LLM judges. While this approach effectively mitigates contamination and judge bias, it remains limited to domains with available structured question sets and focuses on multiple-choice formats rather than completion tasks. Our work introduces a fully deterministic pipeline that automatically converts raw domain corpora directly into completion-type benchmarks without human curation or LLM generation. This approach enables a more accurate evaluation of domain-specific knowledge in base models while scaling efficiently across arbitrary domains.

4.2 Knowledge Attribute and Representation in Language Models

The second part of our analysis focuses on understanding the change in knowledge representation during adaptive pre-training. Initial work in language models has treated them as black boxes, focusing on performance evaluation through external metrics rather than studying the internal representations ([Wang et al., 2018](#); [Gururangan et al., 2021](#)). With the increased model complexity, the work shifted to understanding the internal representation and knowledge storage. With pioneering work by [Rogers et al. \(2021\)](#) and [Tenney et al. \(2019\)](#) demonstrated that the transformers-based models organize the information in a hierarchical format with earlier layer capturing syntactic information and later one more focused on semantics highlighting the non-uniform distribution and unique role of each layer. Later work by [Meng et al. \(2022\)](#) and [Geva et al. \(2020\)](#) further explored where the factual knowledge is stored in LLMs and found them to be predominantly in feed-forward network (FFN) components rather than attention heads, also establishing the FFNs as key-value memory structures that are responsible for storing and retrieving information during inference. [Dai et al. \(2021\)](#) reinforced this understanding, showing that individual neurons within FFNs activate in response to specific concepts or entities. [Dar et al. \(2022\)](#) and [nostalgebraist \(2020\)](#) have further analyzed the distribution of knowledge across model layers, revealing the building up of knowledge as the token progresses through layers and making the layer information progression more transparent. [Geva et al. \(2023\)](#) highlighted the specialized architectural component in knowledge representation, demonstrating that the early MLP layers contribute majorly to subject enrichment while upper multi-head self-attention (MHSA) sublayers perform attribute extraction. Despite these advances, a significant gap remained in understanding how the knowledge representation evolves during domain adaptation. Studies by [Houlsby et al. \(2019\)](#) and [Hu et al. \(2022\)](#) examined parameter-efficient adaptation methods, and [Kirkpatrick et al. \(2017\)](#) studied catastrophic forgetting in continual learning scenarios. Still, they do not focus on the changes inside the model at the activation level but only on the output metric of interest. The closest work to our research is the early work by [Merchant et al. \(2020\)](#), which provides valuable insight into the changes in BERT’s representations across layers during fine-tuning, demonstrating that the linguistic features are maintained while task-specific changes occur primarily in the upper layers. However, to our knowledge, a comprehensive understanding of tracking the effect of domain adaptation and knowledge attribute evolution through layers is lacking. Our work addresses this gap by building on [Geva et al. \(2023\)](#), providing insights into the layerwise transformations and probability distributions during adaptation.

5 Conclusion

In this work, we have addressed the critical challenge of automatic benchmark creation from an arbitrary text corpus and employed this approach to understand the knowledge evolution during both general pre-training and domain adaptation. In Part 1, we have introduced a deterministic pipeline, which, given a raw text corpus, creates a completion-type benchmark without relying on LLMs or human curation. Our pipeline eliminates biases in benchmark creation and prevents benchmark contamination issues by enabling benchmark generation on newly available data. We introduced median rank as a practical metric to evaluate models on our benchmarks. Unlike alternative metrics such as perplexity or last layer attribute rate, our approach strongly correlated with benchmarks created by a state-of-the-art model (Claude 3.7 Sonnet) and showed the expected behavior for intuitive tasks. Notably, we found that the significant improvement in domain adaptation happens for smaller models within shorter training horizons than assumed. We further showed that our method could help evaluate LLMs during pre-training without requiring a few-shot prompts or instruction fine-tuning. These

results have profound implications for finding the most suitable model for the domain of interest and early stopping model training in case of knowledge saturation, saving substantial computational costs by replacing the traditional perplexity metric for domain-specific tasks.

In part 2, we extended the previous work on the layerwise analysis of attribute extraction in LLMs to a domain-adaptive pre-training setting. By incorporating layer norms, we provided smoother and more interpretable insight into the knowledge progression between layers. We discovered that significant changes during domain adaptation happen from initial to mid layers, indicating the importance of these layers in knowledge extraction and enhancing the attributes of input tokens. We also found that the later layer focuses more on the next token prediction and amplifies any knowledge changes from earlier layers, making forgetting effects more pronounced during domain transitions. Our findings can help target specific layers to mitigate forgetting during domain adaptation and guide more targeted and efficient fine-tuning approaches. Future work could extend in this direction to test the effectiveness of freezing the weights of the components identified by our approach and expand our method in a continual learning setting, developing further insight into effective domain adaptation methods.

Acknowledgements Çağatay Yıldız is a member of the Machine Learning Cluster of Excellence, funded by the Deutsche Forschungsgemeinschaft (DFG, German Research Foundation) under Germany’s Excellence Strategy – EXC number 2064/1 – Project number 390727645. This research utilized compute resources at the Tübingen Machine Learning Cloud, DFG FKZ INST 37/1057-1 FUGG.

References

- Anthropic (2025). Claude models. Accessed: March 30, 2025.
- Brown, T., Mann, B., Ryder, N., Subbiah, M., Kaplan, J. D., Dhariwal, P., Neelakantan, A., Shyam, P., Sastry, G., Askell, A., et al. (2020). Language models are few-shot learners. *Advances in neural information processing systems*, 33:1877–1901.
- Chang, Y., Wang, X., Wang, J., Wu, Y., Yang, L., Zhu, K., Chen, H., Yi, X., Wang, C., Wang, Y., et al. (2024). A survey on evaluation of large language models. *ACM transactions on intelligent systems and technology*, 15(3):1–45.
- Chavan, A., Magazine, R., Kushwaha, S., Debbah, M., and Gupta, D. (2024). Faster and lighter llms: A survey on current challenges and way forward. *arXiv preprint arXiv:2402.01799*.
- Chen, S., Wong, S., Chen, L., and Tian, Y. (2023). Extending context window of large language models via positional interpolation. *arXiv preprint arXiv:2306.15595*.
- Computer, T. (2023). Redpajama: An open source recipe to reproduce llama training dataset.
- Cui, S., Yu, S., Huang, H.-Y., Lin, Y.-C.-D., Huang, Y., Zhang, B., Xiao, J., Zuo, H., Wang, J., Li, Z., et al. (2025). mirtarbase 2025: updates to the collection of experimentally validated microRNA–target interactions. *Nucleic Acids Research*, 53(D1):D147–D156.
- Dai, D., Dong, L., Hao, Y., Sui, Z., Chang, B., and Wei, F. (2021). Knowledge neurons in pretrained transformers. *arXiv preprint arXiv:2104.08696*.
- Dai, Z., Yang, Z., Yang, Y., Carbonell, J., Le, Q. V., and Salakhutdinov, R. (2019). Transformer-xl: Attentive language models beyond a fixed-length context. *arXiv preprint arXiv:1901.02860*.
- Dao, T., Fu, D., Ermon, S., Rudra, A., and Ré, C. (2022). Flashattention: Fast and memory-efficient exact attention with io-awareness. *Advances in neural information processing systems*, 35:16344–16359.
- Dar, G., Geva, M., Gupta, A., and Berant, J. (2022). Analyzing transformers in embedding space. *arXiv preprint arXiv:2209.02535*.
- Ding, J., Ma, S., Dong, L., Zhang, X., Huang, S., Wang, W., Zheng, N., and Wei, F. (2023). Longnet: Scaling transformers to 1,000,000,000 tokens. *arXiv preprint arXiv:2307.02486*.

- Frantar, E., Ashkboos, S., Hoefler, T., and Alistarh, D.-A. (2023). Optq: Accurate post-training quantization for generative pre-trained transformers. In *11th International Conference on Learning Representations*.
- Gehrmann, S., Adewumi, T., Aggarwal, K., Ammanamanchi, P. S., Anuoluwapo, A., Bosselut, A., Chandu, K. R., Clinciu, M., Das, D., Dhole, K. D., et al. (2021). The gem benchmark: Natural language generation, its evaluation and metrics. *arXiv preprint arXiv:2102.01672*.
- Geva, M., Bastings, J., Filippova, K., and Globerson, A. (2023). Dissecting recall of factual associations in auto-regressive language models. *arXiv preprint arXiv:2304.14767*.
- Geva, M., Schuster, R., Berant, J., and Levy, O. (2020). Transformer feed-forward layers are key-value memories. *arXiv preprint arXiv:2012.14913*.
- Gu, A. and Dao, T. (2023). Mamba: Linear-time sequence modeling with selective state spaces. *arXiv preprint arXiv:2312.00752*.
- Gururangan, S., Lewis, M., Holtzman, A., Smith, N. A., and Zettlemoyer, L. (2021). Demix layers: Disentangling domains for modular language modeling. *arXiv preprint arXiv:2108.05036*.
- Han, T., Adams, L. C., Papaioannou, J.-M., Grundmann, P., Oberhauser, T., Löser, A., Truhn, D., and Bressen, K. K. (2023). Medalpaca—an open-source collection of medical conversational ai models and training data. *arXiv preprint arXiv:2304.08247*.
- Hendrycks, D., Burns, C., Basart, S., Zou, A., Mazeika, M., Song, D., and Steinhardt, J. (2020). Measuring massive multitask language understanding. *arXiv preprint arXiv:2009.03300*.
- Houlsby, N., Giurugu, A., Jastrzebski, S., Morrone, B., De Laroussilhe, Q., Gesmundo, A., Attariyan, M., and Gelly, S. (2019). Parameter-efficient transfer learning for nlp. In *International conference on machine learning*, pages 2790–2799. PMLR.
- Hu, E. J., Shen, Y., Wallis, P., Allen-Zhu, Z., Li, Y., Wang, S., Wang, L., Chen, W., et al. (2022). Lora: Low-rank adaptation of large language models. *ICLR*, 1(2):3.
- Hu, J., Dong, T., Gang, L., Ma, H., Zou, P., Sun, X., Guo, D., Yang, X., and Wang, M. (2024). Psycollm: Enhancing llm for psychological understanding and evaluation. *IEEE Transactions on Computational Social Systems*.
- Imani, S., Du, L., and Shrivastava, H. (2023). Mathprompter: Mathematical reasoning using large language models. *arXiv preprint arXiv:2303.05398*.
- Jelinek, F., Mercer, R. L., Bahl, L. R., and Baker, J. K. (1977). Perplexity—a measure of the difficulty of speech recognition tasks. *The Journal of the Acoustical Society of America*, 62(S1):S63–S63.
- Kaplan, J., McCandlish, S., Henighan, T., Brown, T. B., Chess, B., Child, R., Gray, S., Radford, A., Wu, J., and Amodei, D. (2020). Scaling laws for neural language models. *arXiv preprint arXiv:2001.08361*.
- Kirkpatrick, J., Pascanu, R., Rabinowitz, N., Veness, J., Desjardins, G., Rusu, A. A., Milan, K., Quan, J., Ramalho, T., Grabska-Barwinska, A., et al. (2017). Overcoming catastrophic forgetting in neural networks. *Proceedings of the national academy of sciences*, 114(13):3521–3526.
- Lai, J., Gan, W., Wu, J., Qi, Z., and Philip, S. Y. (2024). Large language models in law: A survey. *AI Open*.
- Lewis, P., Stenetorp, P., and Riedel, S. (2020). Question and answer test-train overlap in open-domain question answering datasets. *arXiv preprint arXiv:2008.02637*.
- Li, T., Zhang, G., Do, Q. D., Yue, X., and Chen, W. (2024). Long-context llms struggle with long in-context learning. *arXiv preprint arXiv:2404.02060*.
- Li, Y., Wang, S., Ding, H., and Chen, H. (2023). Large language models in finance: A survey. In *Proceedings of the fourth ACM international conference on AI in finance*, pages 374–382.

- Liu, L., Cui, G., Wan, C., Wu, D., and Li, Y. (2024). Ecg-llm: Leveraging large language models for low-quality ecg signal restoration. In *2024 IEEE International Conference on Bioinformatics and Biomedicine (BIBM)*, pages 3537–3542. IEEE.
- Lo, K., Wang, L. L., Neumann, M., Kinney, R., and Weld, D. S. (2019). S2orc: The semantic scholar open research corpus. *arXiv preprint arXiv:1911.02782*.
- Meister, C. and Cotterell, R. (2021). Language model evaluation beyond perplexity. *arXiv preprint arXiv:2106.00085*.
- Meng, K., Bau, D., Andonian, A., and Belinkov, Y. (2022). Locating and editing factual associations in gpt. *Advances in neural information processing systems*, 35:17359–17372.
- Merchant, A., Rahimtoroghi, E., Pavlick, E., and Tenney, I. (2020). What happens to bert embeddings during fine-tuning? *arXiv preprint arXiv:2004.14448*.
- Monea, G., Peyrard, M., Josifoski, M., Chaudhary, V., Eisner, J., Kıcıman, E., Palangi, H., Patra, B., and West, R. (2023). A glitch in the matrix? locating and detecting language model grounding with fakepedia. *arXiv preprint arXiv:2312.02073*.
- Nam, D., Macvean, A., Hellendoorn, V., Vasilescu, B., and Myers, B. (2024). Using an llm to help with code understanding. In *Proceedings of the IEEE/ACM 46th International Conference on Software Engineering*, pages 1–13.
- Nguyen, T. D., Ting, Y.-S., Ciucă, I., O’Neill, C., Sun, Z.-C., Jabłońska, M., Kruk, S., Perkowski, E., Miller, J., Li, J., et al. (2023). Astrollama: Towards specialized foundation models in astronomy. *arXiv preprint arXiv:2309.06126*.
- nostalgebraist (2020). Interpreting GPT: the logit lens.
- Öncel, F., Bethge, M., Ermis, B., Ravanelli, M., Subakan, C., and Yıldız, Ç. (2024). Adaptation odyssey in llms: Why does additional pretraining sometimes fail to improve? *arXiv preprint arXiv:2410.05581*.
- Pedregosa, F., Varoquaux, G., Gramfort, A., Michel, V., Thirion, B., Grisel, O., Blondel, M., Prettenhofer, P., Weiss, R., Dubourg, V., et al. (2011). Scikit-learn: Machine learning in python. *the Journal of machine Learning research*, 12:2825–2830.
- Perez, E., Ringer, S., Lukosiute, K., Nguyen, K., Chen, E., Heiner, S., Pettit, C., Olsson, C., Kundu, S., Kadavath, S., et al. (2023). Discovering language model behaviors with model-written evaluations. In *Findings of the Association for Computational Linguistics: ACL 2023*, pages 13387–13434.
- Qin, Y., Zhang, J., Lin, Y., Liu, Z., Li, P., Sun, M., and Zhou, J. (2022). Elle: Efficient lifelong pre-training for emerging data. *arXiv preprint arXiv:2203.06311*.
- Reid, M., Zhong, V., Gururangan, S., and Zettlemoyer, L. (2022). M2d2: A massively multi-domain language modeling dataset. *arXiv preprint arXiv:2210.07370*.
- Rogers, A., Kovaleva, O., and Rumshisky, A. (2021). A primer in bertology: What we know about how bert works. *Transactions of the association for computational linguistics*, 8:842–866.
- Sharma, P., Ash, J. T., and Misra, D. (2023). The truth is in there: Improving reasoning in language models with layer-selective rank reduction. *arXiv preprint arXiv:2312.13558*.
- Siriwardhana, S., McQuade, M., Gauthier, T., Atkins, L., Neto, F. F., Meyers, L., Vij, A., Odenthal, T., Goddard, C., MacCarthy, M., et al. (2024). Domain adaptation of llama3-70b-instruct through continual pre-training and model merging: A comprehensive evaluation. *arXiv preprint arXiv:2406.14971*.
- Srivastava, A., Rastogi, A., Rao, A., Shoeb, A. A. M., Abid, A., Fisch, A., Brown, A. R., Santoro, A., Gupta, A., Garriga-Alonso, A., et al. (2022). Beyond the imitation game: Quantifying and extrapolating the capabilities of language models. *arXiv preprint arXiv:2206.04615*.

- Tenney, I., Das, D., and Pavlick, E. (2019). Bert rediscovers the classical nlp pipeline. *arXiv preprint arXiv:1905.05950*.
- Tian, D., Jiang, S., Zhang, L., Lu, X., and Xu, Y. (2023). The role of large language models in medical image processing: a narrative review. *Quantitative Imaging in Medicine and Surgery*, 14(1):1108.
- Touvron, H., Martin, L., Stone, K., Albert, P., Almahairi, A., Babaei, Y., Bashlykov, N., Batra, S., Bhargava, P., Bhosale, S., et al. (2023). Llama 2: Open foundation and fine-tuned chat models. *arXiv preprint arXiv:2307.09288*.
- Wang, A., Pruksachatkun, Y., Nangia, N., Singh, A., Michael, J., Hill, F., Levy, O., and Bowman, S. (2019). Superglue: A stickier benchmark for general-purpose language understanding systems. *Advances in neural information processing systems*, 32.
- Wang, A., Singh, A., Michael, J., Hill, F., Levy, O., and Bowman, S. R. (2018). Glue: A multi-task benchmark and analysis platform for natural language understanding. *arXiv preprint arXiv:1804.07461*.
- Wang, H., Zhao, S., Qiang, Z., Xi, N., Qin, B., and Liu, T. (2024). Beyond direct diagnosis: Llm-based multi-specialist agent consultation for automatic diagnosis. *arXiv preprint arXiv:2401.16107*.
- White, C., Dooley, S., Roberts, M., Pal, A., Feuer, B., Jain, S., Shwartz-Ziv, R., Jain, N., Saifullah, K., Naidu, S., et al. (2024). Livebench: A challenging, contamination-free llm benchmark. *arXiv preprint arXiv:2406.19314*.
- Xie, Y., Aggarwal, K., and Ahmad, A. (2024). Efficient continual pre-training for building domain specific large language models. In *Findings of the Association for Computational Linguistics ACL 2024*, pages 10184–10201.
- Xu, Z., Gupta, A., Li, T., Bentham, O., and Srikumar, V. (2024). Beyond perplexity: Multi-dimensional safety evaluation of llm compression. *arXiv preprint arXiv:2407.04965*.
- Yıldız, Ç., Ravichandran, N. K., Punia, P., Bethge, M., and Ermis, B. (2024). Investigating continual pretraining in large language models: Insights and implications. *arXiv preprint arXiv:2402.17400*.
- Yuan, P., Feng, S., Li, Y., Wang, X., Zhang, Y., Shi, J., Tan, C., Pan, B., Hu, Y., and Li, K. (2025). Llm-powered benchmark factory: Reliable, generic, and efficient. *arXiv preprint arXiv:2502.01683*.
- Zhou, K., Zhu, Y., Chen, Z., Chen, W., Zhao, W. X., Chen, X., Lin, Y., Wen, J.-R., and Han, J. (2023). Don’t make your llm an evaluation benchmark cheater. *arXiv preprint arXiv:2311.01964*.

A Supplementary Material

A.1 Sample Document from Dataset

Below we present a sample document from our arXiv and Kaggle dataset after mapping, showing both the metadata and the beginning of the full-text content:

Title: Hoffmann-Ostenhof's conjecture for traceable cubic graphs

Categories: math.CO cs.DM

Abstract: In 2011 Hoffmann-Ostenhof proposed the following conjecture: Every connected cubic graph can be decomposed into a spanning tree, a matching and a family of cycles. In this paper we prove that this conjecture holds for traceable cubic graphs.

Introduction: Let G be a simple undirected graph with the *vertex set* $V(G)$ and the *edge set* $E(G)$. A vertex with degree one is called a *pendant vertex*. The distance between the vertices u and v in graph G is denoted by $d_G(u, v)$. A cycle C is called *chordless* if C has no *cycle chord* (that is an edge not in the edge set of C whose endpoints lie on the vertices of C). The *Induced subgraph* on vertex set S is denoted by $\langle S \rangle$. A path that starts in v and ends in u is denoted by \widehat{vu} . A *traceable* graph is a graph that possesses a Hamiltonian path. In a graph G , we say that a cycle C is *formed by the path* Q if $|E(C) \setminus E(Q)| = 1$. So every vertex of C belongs to $V(Q)$...

Our dataset contains 1.56 million documents with similar structures, covering the full spectrum of scientific disciplines represented in arXiv.

Table 1: Example of 3 keywords, first 10 elements from word-list (TF and TF-IDF), and first 15 tokens from tokenizers (GPT2-XL, LLAMA-2 7B, OLMo-2 7B) for CS.AI domain.

Keyword	Word-list (TF)	Word-list (TF-IDF)	Token list
machine learning	learning, machine, data, algorithms, Machine, models, Learning, methods, model, used	International, Conference, Forest, Logistic, Naive, forests, forest, Forests, Trees, Proceedings	GPT2-XL: learning, machine, data, algorithms, Machine, models, Learning, methods, model, used, techniques, supervised, classification, problem, algorithm LLAMA-2 7B: learning, machine, data, algorithms, Machine, models, vised, model, super, Learning, methods, ing, used, based, techniques OLMo-2 7B: learning, machine, data, algorithms, Machine, models, Learning, model, methods, used, techniques, supervised, algorithm, classification, problem
reinforcement learning	learning, reinforcement, policy, reward, agent, Reinforcement, Learning, model, state, learn	critic, Actor, Inverse, Reward, MDPs, replay, Iteration, bandit, Offline, Atari	GPT2-XL: learning, reinforcement, policy, reward, agent, forcement, Rein, Learning, model, state, function, learn, algorithm, algorithms, problem LLAMA-2 7B: learning, cement, rein, policy, reward, agent, Rein, model, Learning, state, based, function, learn, ing, algorithm OLMo-2 7B: learning, reinforcement, policy, reward, agent, forcement, Rein, Learning, model, state, function, learn, algorithm, algorithms, problem
policy optimization	policy, learning, optimal, policies, algorithm, reinforcement, reward, gradient, optimization, agent	critic, Proximal, Actor, MDPs, PPO, Deterministic, Bellman, discounted, DDPG, regret	GPT2-XL: learning, reinforcement, policy, reward, agent, forcement, Rein, Learning, model, state, function, learn, algorithm, algorithms, problem LLAMA-2 7B: learning, cement, rein, policy, reward, agent, Rein, model, Learning, state, based, function, learn, ing, algorithm OLMo-2 7B: learning, reinforcement, policy, reward, agent, forcement, Rein, Learning, model, state, function, learn, algorithm, algorithms, problem

Table 2: Prompt and corresponding target for given keywords from Computer Science - Artificial Intelligence (CS.AI) and Physics and Society (physics.soc-ph) domains.

Keyword	Prompt	Target
Domain: Computer Science - Artificial Intelligence (CS.AI)		
Neural Networks	Neural networks are usually trained using some variation of	backpropagation
Neural Networks	We use neural networks as surrogates for the solution	function
Reinforcement Learning	The agent aims to learn the policies in an on-line manner which requires efficiently balancing exploration of state-space and	exploitation
Reinforcement Learning	A central challenge in reinforcement learning (RL) is designing agents which can solve complex, long-horizon	tasks
Machine Learning	The main components of Machine Learning are: tasks,	models
Machine Learning	These systems are usually based on a Machine Learning (ML)	model
Domain: Physics and Society (physics.soc-ph)		
Community Detection Algorithms	To explore the value of using bipartite information in community	detection
Community Detection Algorithms	We thus conjecture that standard community detection algorithms have difficulty	detecting
Social Network	For instance, in social networks individuals can belong to different circles at the same time, like family,	friends
Social Network	Understanding the structure of such networks has become essential since the structure affects their performance, for example the topology of social networks	influences
Complex Networks	Most social, biological, and technological networks (including the brain) display substantial non-trivial	topological
Complex Networks	The network exhibit a clear core-periphery structure, with a core of densely	interconnected

A.2 Smaller Language Models and Few-Shot Learning: An Example for GPT2-XL Model

To demonstrate the sensitivity to few-shot learning faced in smaller language models, we take one example for the GPT2-XL model. We tested GPT-2 XL on simple geography questions using greedy decoding (`do_sample=False`, `num_beams=1`).

When presented with a single question, GPT-2 XL demonstrated correct factual knowledge:

Prompt 1

Question: Which of the following is the capital of France?

- A) Berlin
- B) Madrid
- C) Paris
- D) Rome

Answer:

For this prompt, GPT-2 XL correctly completed with “C”, identifying Paris. However, when presented with a sequence of questions in a few-shot format:

Prompt 2

Question: Which of the following is the capital of Germany?

- A) Paris
- B) Berlin
- C) Warsaw
- D) Vienna

Answer: B

Question: Which of the following is the capital of Italy?

- A) Madrid
- B) Athens
- C) Rome
- D) Lisbon

Answer: C

Question: Which of the following is the capital of Spain?

- A) Rome
- B) Paris
- C) London
- D) Madrid

Answer: D

Question: Which of the following is the capital of France?

- A) Berlin
- B) Madrid
- C) Rome
- D) Paris

Answer:

The model incorrectly completed with “B” (Madrid), despite being able to answer correctly when prompted without a few-shot prompt. This inconsistency highlights how smaller base models can sometimes fail to properly utilize in-context examples, reinforcing the need for our more structured approach to knowledge testing that reduces formatting sensitivity.

A.3 Cosine Similarity Between Targets and Computer Science Phrase for GPT2-XL Adaptive Training

To measure the relevance of the targets predicted better by the CS.AI domain-trained model as compared to the base model. We developed a token-level model comparison metric that addresses several

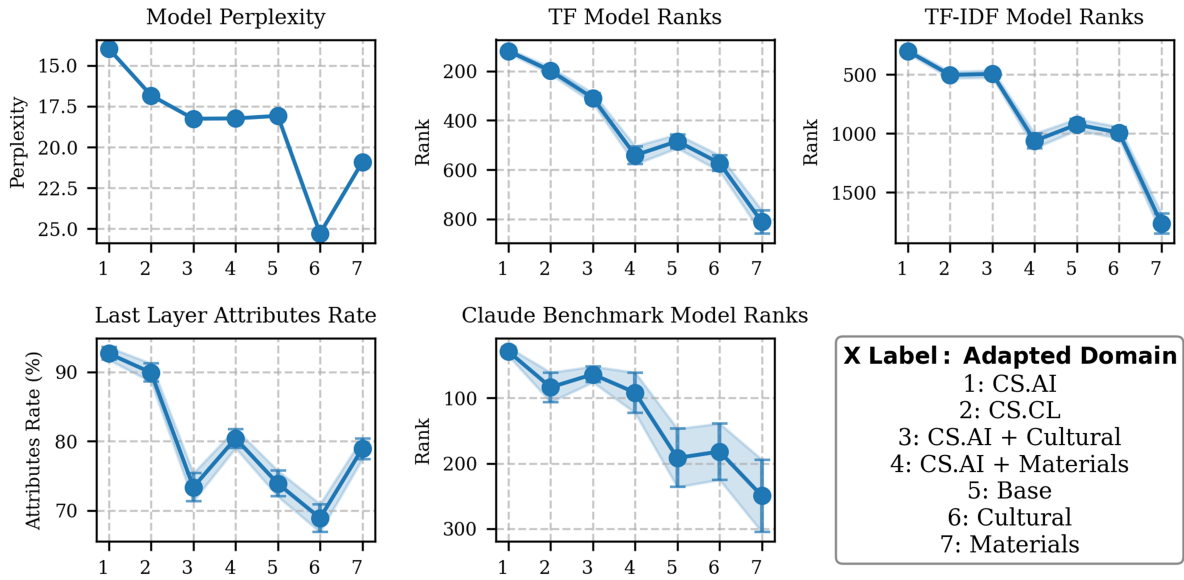


Figure 13: Mean values instead of median for Figure 2 for domain adaptation for GPT2-XL on six domains. We can see the trend is almost similar to the one described in the median figure, but here, the values on the y-axis are larger for ranks as it also includes the outliers.

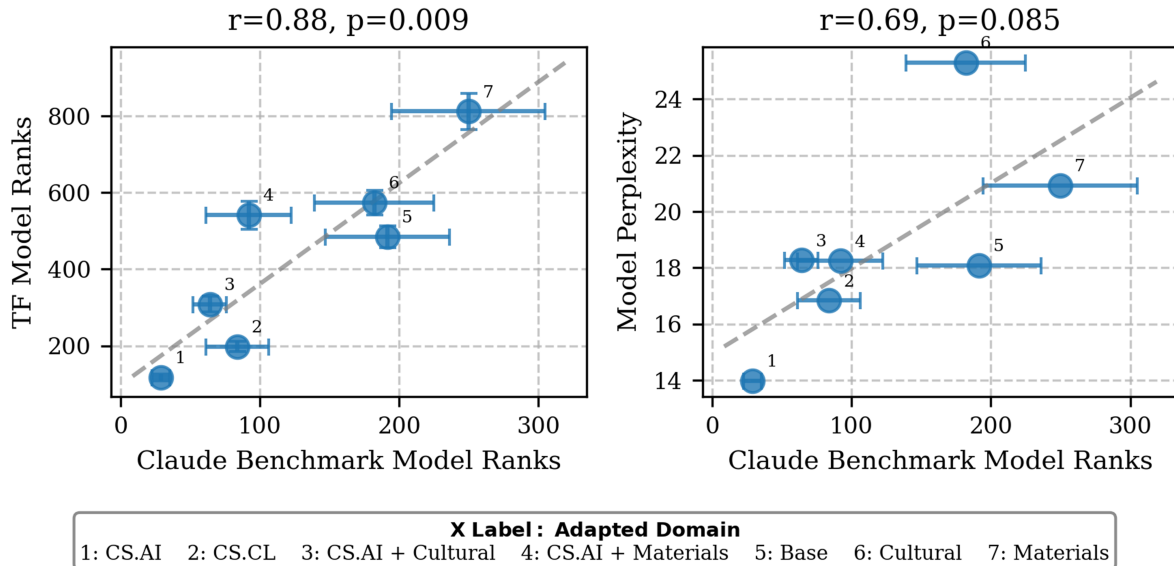


Figure 14: Correlation for the mean plot Figure 13 between Claude benchmark and TF ranks and perplexity for the GPT2-XL model adaptive on six domains, including the base model. We can see a significant correlation for the mean TF rank as well.

Table 3: Tokens with highest and lowest performance improvements in the CS.AI domain-trained model

Top 100 Tokens	Bottom 100 Tokens
Policy, Answer, tracing, margin, bases, policy, actions, baselines, answer, answering, Critic, action, planner, reward, Error, prediction, agent, explainability, MDP, generalization, weakly, critic, graphs, proposed, contrastive, efficiency, paper, Interpretable, Diversity, exploration, partially, approximate, Recall, Logic, learnt, Monte, Support, Atari, labeled, continual, Search, Partially, training, steps, segmentation, Inverse, Mixed, NMT, distillation, detection, Markov, reinforcement, best, interacting, states, classifiers, adaptation, loss, segment, UAV, Context, homogeneous, Explainable, policies, federated, demonstration, discriminator, language, Freebase, commonsense, unsupervised, control, rewards, PSO, diarization, tabular, differentiable, Table, privacy, entities, made, regularization, intersection, complexity, agents, publicly, mentions, natural, matching, spaces, relations, catastrophic, research, intrusion, program, SNNs, systems, DDPG, future, confident	parsing, one, like, discuss, Multivariate, Tree, destination, understanding, autoencoders, sensor, outliers, squared, offensive, structures, percent, languages, MRI, drones, science, score, video, fields, explainers, public, ODE, credit, SGD, may, decoder, vertices, logistic, contains, transitions, problem, Generation, backpropagate, drive, output, attacks, world, allocating, trials, sources, magnetic, size, implementation, field, signals, behavior, analysis, protect, cards, non-linear, Absolute, Science, way, PDEs, strategy, land, emotional, percentage, French, improved, dimensionality, classical, observation, hyperparameters, Facebook, percents, private, example, theoretical, syntactic, domain, Code, bound, analogy, MCMC, explainer, truth, multivariate, layer, mergers, PDE, protection, fMRI, multivariable, imaging, media, direction, allocate, MRIs, Anomaly, government, boxes, ratio, equations, FMRI, chart, differential

Note: Tokens are listed in descending order of performance improvement as measured by the composite weighted metric. The top tokens show significantly higher semantic similarity to the CS.AI domain ($p = 2.82e-05$, Cohen’s $d = 0.31$).

limitations in standard evaluation approaches. First, we computed both probability and rank differences between our CS.AI model and baseline models for each target token. To account for scale bias in probability differences and to balance the influence of both metrics, we created a composite score by normalizing both probability and rank improvements to equal scales and giving them equal weight (50% each). Recognizing that token frequency can distort analysis by over-emphasizing rare tokens with extreme differences, we applied a logarithmic frequency weighting to this composite score. The resulting composite weighted metric emphasizes improvements on commonly occurring tokens while maintaining sensitivity to meaningful differences in rare but potentially essential tokens. We employed the all-MiniLM-L6-v2 sentence transformer for semantic analysis to embed each token and the reference domain term "Computer Science Artificial Intelligence" into a shared vector space, calculating cosine similarity to quantify domain relevance. Statistical significance between the top and bottom performance groups was assessed using independent samples t-tests with Cohen’s d for effect size quantification. Figure 3 shows a semantic alignment between CS.AI’s performance and specialized domain knowledge. Tokens, where CS.AI performed better (top 25% by composite_weighted score), showed significantly higher semantic similarity to "Computer Science Artificial Intelligence" compared to tokens with the lowest performance ($p = 2.82e-05$, Cohen’s $d = 0.31$). Domain-specific terms like "classifiers," "algorithms," and "program" clustered in the high-performance group, while semantically distant terms like "fMRI" and "boxes" appeared mainly in the low-performance group. The violin distributions reveal different central tendencies and variance patterns between groups. Importantly, token frequency (shown by point size) was distributed across both similarity ranges, confirming our weighting approach successfully prevented frequency bias from dominating the analysis. Complete lists of the top and bottom 100 tokens further support this finding (Table 3), with specialized AI terminology concentrated in the high-performance group. These results provide strong evidence that CS.AI has developed genuine domain expertise rather than merely statistical advantages, validating results for our benchmark.

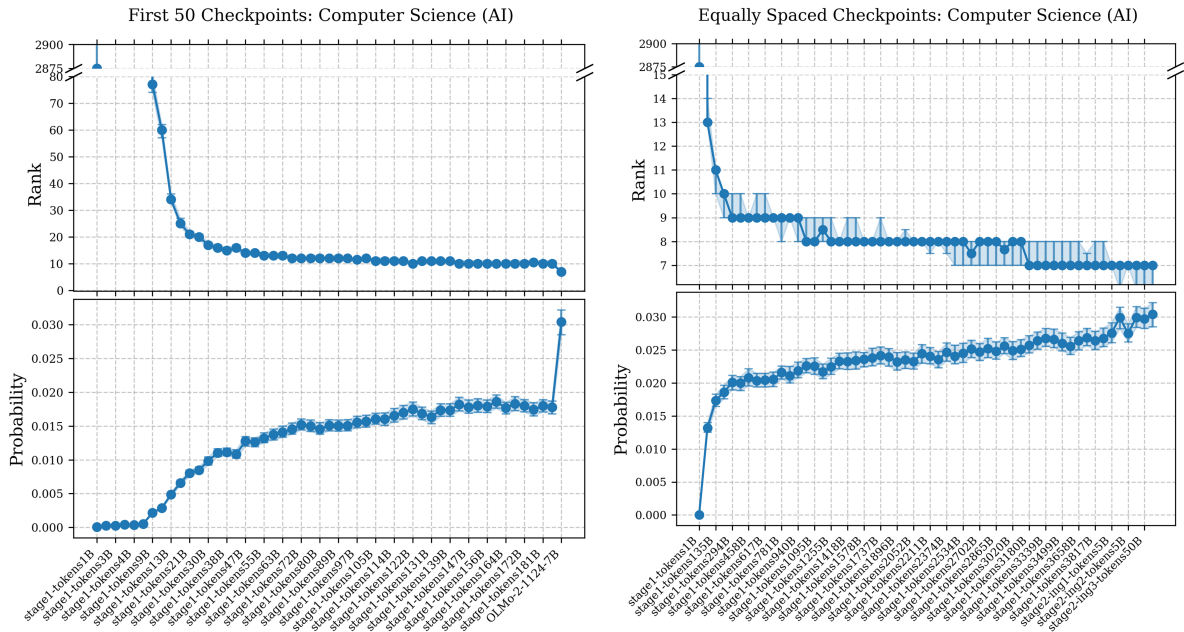


Figure 15: The figure shows the evolution of TF median rank and probability for OLMo-2 checkpoints on the Computer Science – Artificial Intelligence domain from the arXiv dataset. We can observe a similar trend as described in Figure 6. The overall ranks are lower, and probability values higher compared to the Physics and Society domain, indicating the model is relatively better in CS.AI related domain knowledge.

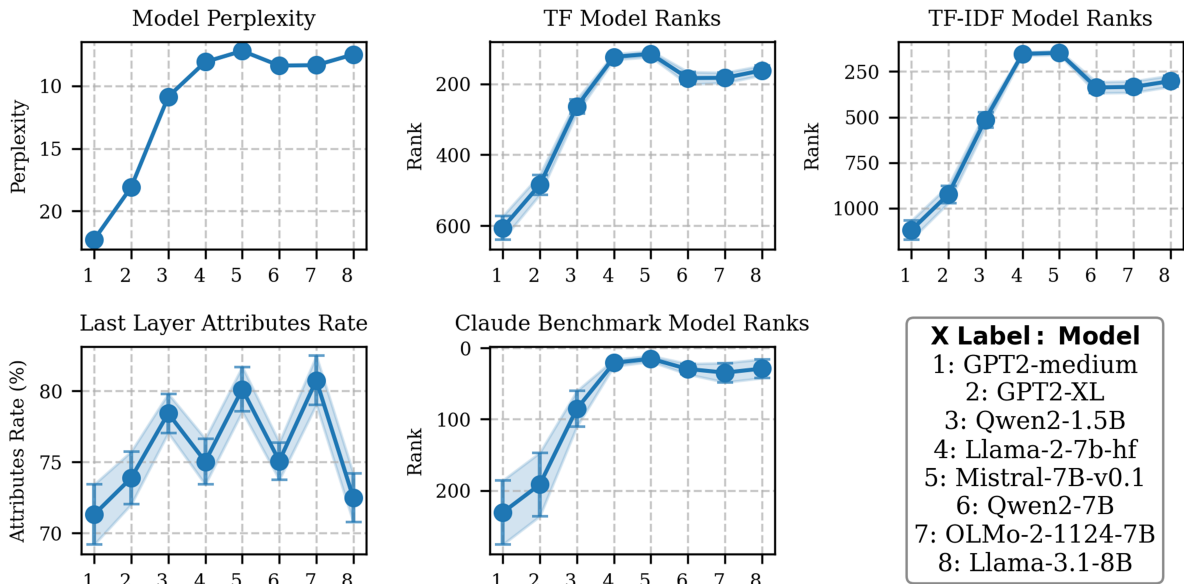


Figure 16: Figure shows the mean ranks, attribute rates, and perplexity values for eight distinct models evaluated on the CS.AI domain. Here, we can similar pattern as seen in the median rank plot but with relatively higher rank values.

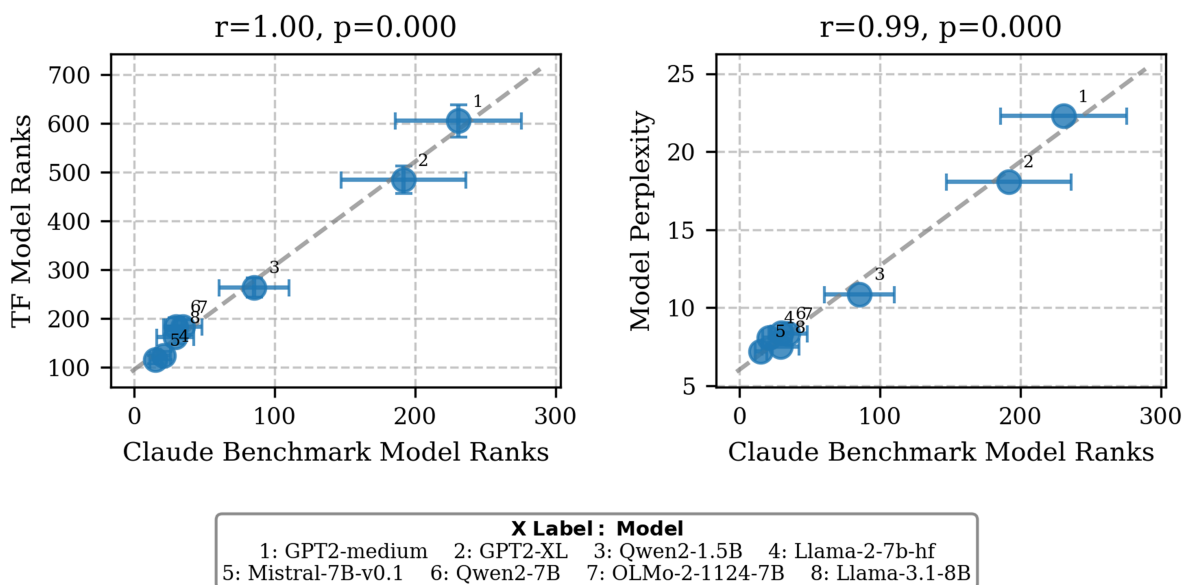


Figure 17: In this correlation plot for Figure 16, we can see an almost perfect correlation between TF model ranks from the arXiv dataset and the ranks from the Claude benchmark.

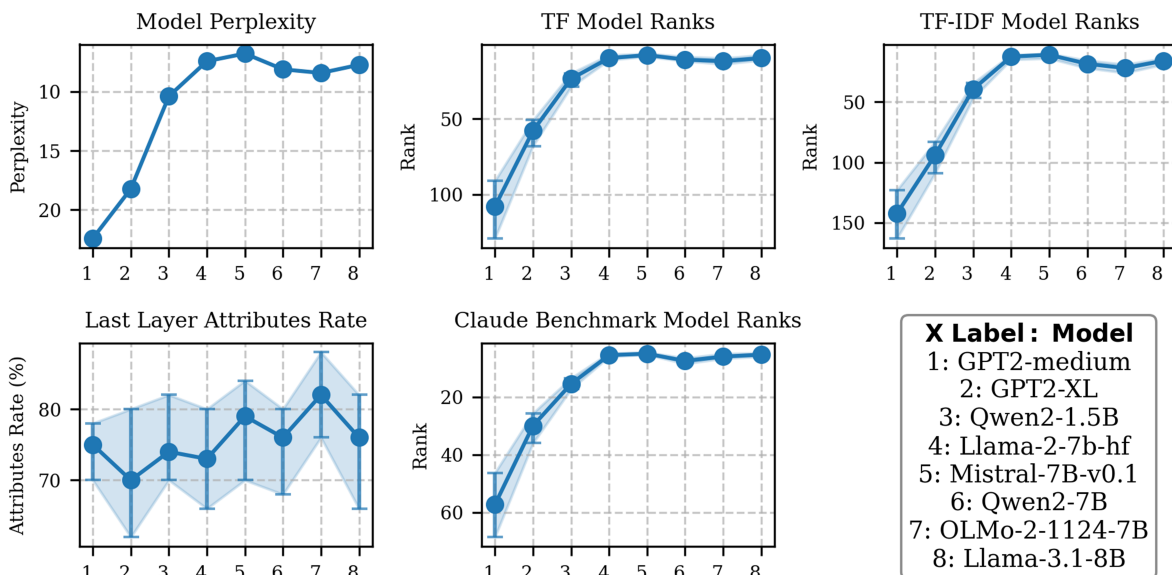


Figure 18: Same figure as Figure 7 for Physics and Society domain. We can see a similar pattern is followed here by almost all the metrics, hence strengthening the results from our previous analysis.

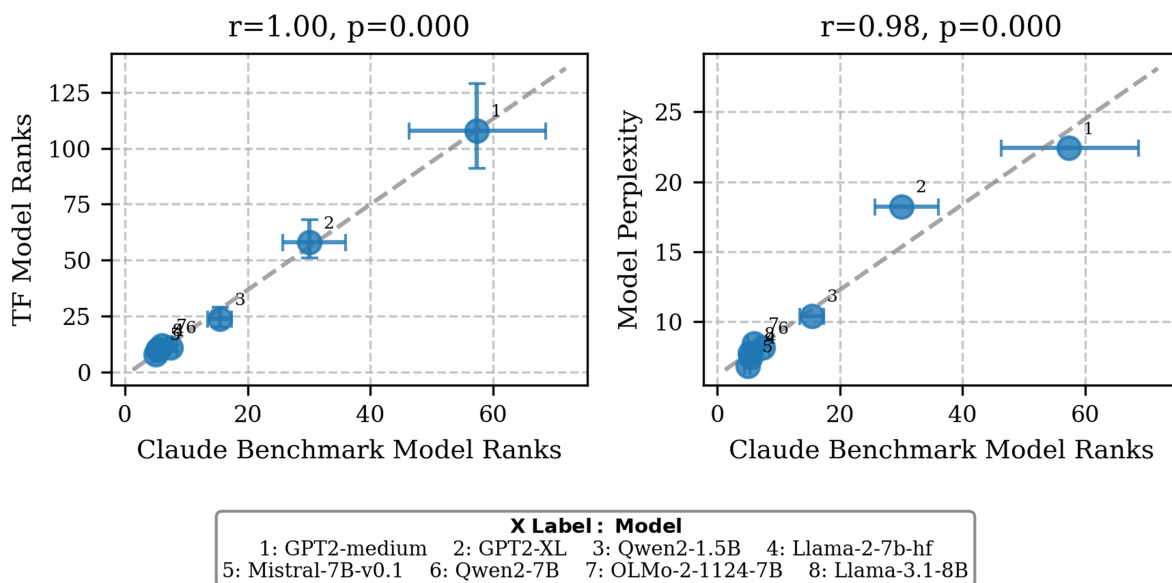


Figure 19: In this correlation plot for Figure 18, and similar to CS.AI domain, here we can conclude similar results fortifying our introduced ranking approach.

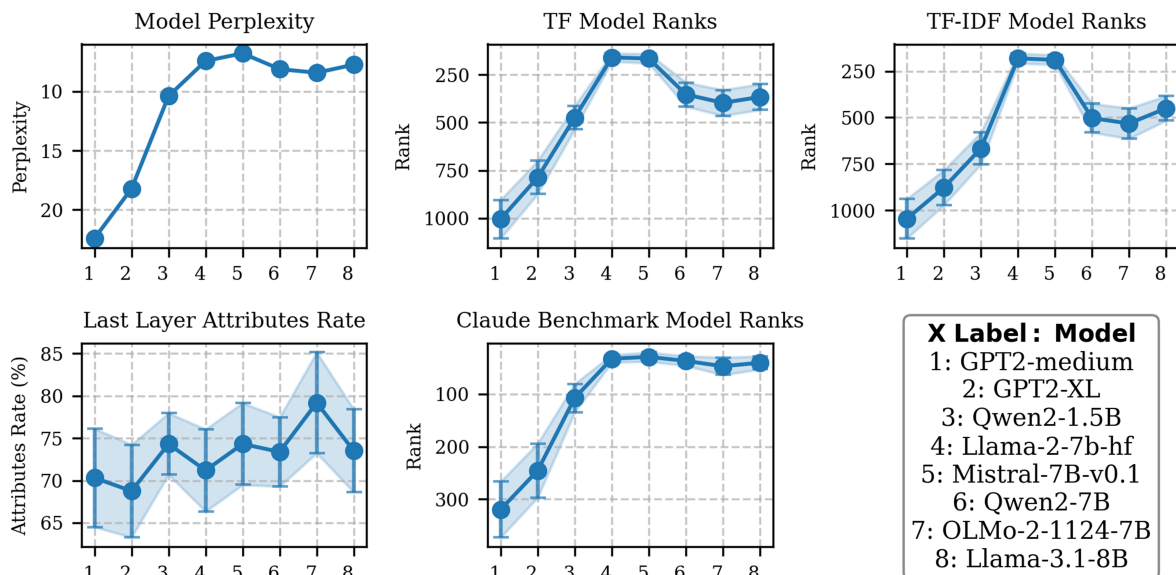
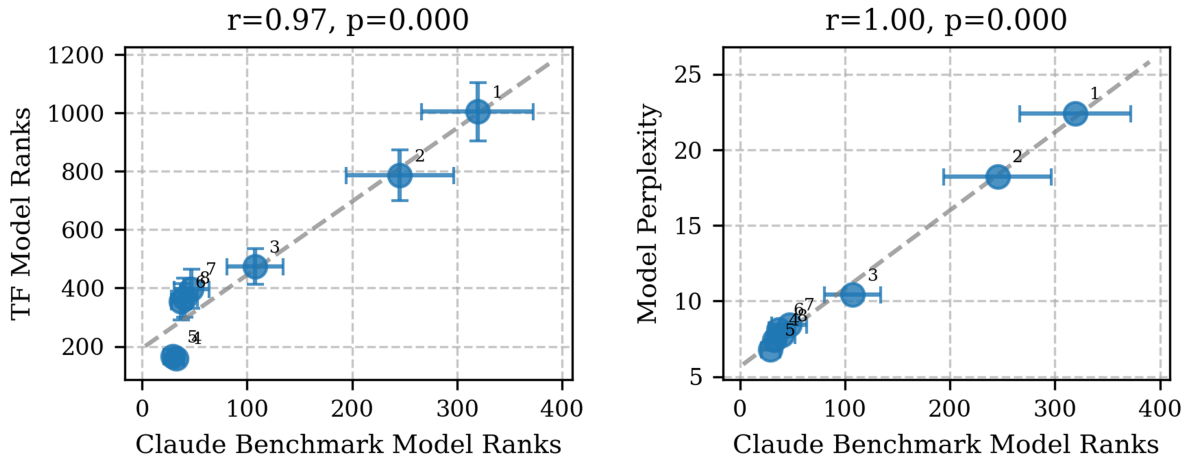


Figure 20: Figure shows the mean ranks, attribute rates, and perplexity values for eight distinct models evaluated on the Physics and Society domain.



X Label : Model
 1: GPT2-medium 2: GPT2-XL 3: Qwen2-1.5B 4: Llama-2-7b-hf
 5: Mistral-7B-v0.1 6: Qwen2-7B 7: OLMo-2-1124-7B 8: Llama-3.1-8B

Figure 21: Correlation plot for Figure 20, where we can see a similar outcome as for the CS.AI domain.

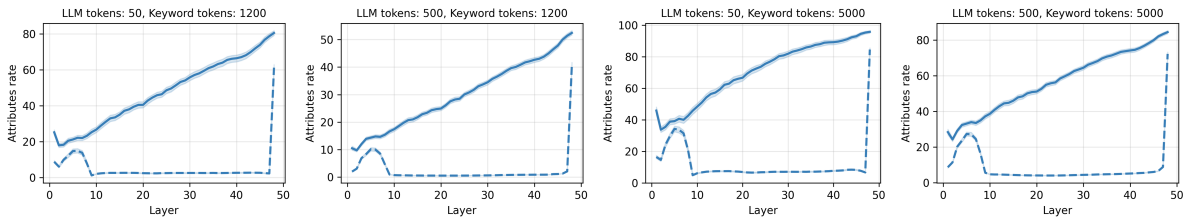


Figure 22: For the GPT2-XL model, we plotted different configurations of LLM tokens and Keyword tokens employed. We can see a similar pattern is followed by each case presented as was shown in the Geva et al. (2023). The changing factor is the attributes rate, which increases with the increase in the pool of keyword-related tokens, because the denominator only consists of LLM tokens in the formula for calculating the attributes rate.

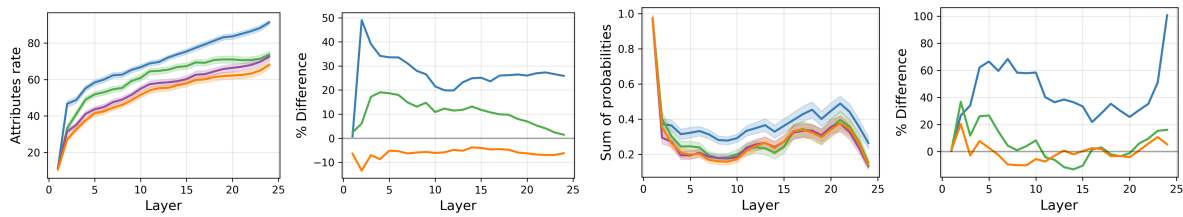


Figure 23: Figure shows the same plot of change in the attributes rate and sum of probability along with the percentage change compared to the base model for GPT-2 medium-adapted models. Although the relative effect is less, the overall trend is consistent with the GPT-2 XL model shown in Figure 11.

Table 4: OLMo-2 checkpoint models used in our analysis

Category	Checkpoint Details	Token Range
First 50	OLMo-2-1124-7B_checkpoint-stage1-step 150(1B), 600(3B), 700(3B), 850(4B), 900(4B), 1000(5B), 2000(9B), 2150(10B), 3000(13B), 4000(17B), 5000(21B), 6000(26B), 7000(30B), 8000(34B), 9000(38B), 10000(42B), 11000(47B), 12000(51B), 13000(55B), 14000(59B), 15000(63B), 16000(68B), 17000(72B), 18000(76B), 19000(80B), 20000(84B), 21000(89B), 22000(93B), 23000(97B), 24000(101B), 25000(105B), 26000(110B), 27000(114B), 28000(118B), 29000(122B), 30000(126B), 31000(131B), 32000(135B), 33000(139B), 34000(143B), 35000(147B), 36000(151B), 37000(156B), 38000(160B), 39000(164B), 40000(168B), 41000(172B), 42000(177B), 43000(181B), 44000(185B)	1B - 185B
Equally Spaced	OLMo-2-1124-7B_checkpoint-stage1-step 150(1B), 13000(55B), 32000(135B), 51000(214B), 70000(294B), 89000(374B), 109000(458B), 128000(537B), 147000(617B), 166000(697B), 186000(781B), 205000(860B), 224000(940B), 242000(1016B), 261000(1095B), 280000(1175B), 299000(1255B), 319000(1338B), 338000(1418B), 357000(1498B), 376000(1578B), 395000(1657B), 414000(1737B), 433000(1817B), 452000(1896B), 470000(1972B), 489000(2052B), 508000(2131B), 527000(2211B), 547000(2295B), 566000(2374B), 585000(2454B), 604000(2534B), 624000(2618B), 644000(2702B), 663000(2781B), 683000(2865B), 701000(2941B), 720000(3020B), 739000(3100B), 758000(3180B), 777000(3259B), 796000(3339B), 815000(3419B), 834000(3499B), 853000(3578B), 872000(3658B), 891000(3738B), 910000(3817B), 928646(3896B) + Stage2-ingredient checkpoints: ingredient1-step1000(5B), ingredient1-step11931(50B), ingredient2-step1000(5B), ingredient2-step11931(50B), ingredient3-step11931(50B)	1B - 3896B
Final Model	OLMo-2-1124-7B	Complete

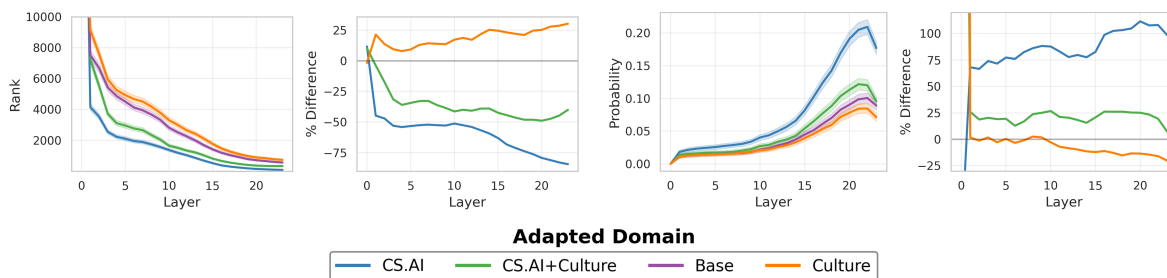


Figure 24: Same analysis as done in Figure 12 for GPT-2 medium model adapted to different domains on m2d2 dataset. We can see that a similar trend is followed here for GPT-2 XL, and overall adaptive training improves both the metrics when the adapted domain aligns with the target domain, with changes happening in both the early phase and later phase.

Table 5: Top 50 tokens predicted by the model for different keywords, categorized by presence in the keyword token list

Keyword	In the token list	Not in the token list
Machine Learning	algorithms, algorithm, models, techniques, systems, model, based, system, methods, framework, technology, software	,, ., and, is, ", to, in, \n, for, (, ",), on, ." with, :, that, has, -, ', can,),, —, or, as, "., ", /, will, —, ;, at,),, from, are, of, [, —
Reinforcement Learning	algorithm, algorithms, model, system, systems, models, based, theory, task	(, ,, ., ", and, \n, ', is, in, ", ;, to, ." with, for,), ",, "., [or, —,),, -, —, ;,], on, ., has, of, ,, that, /, -, ',),, as, ', -, can, from
Deep Learning	algorithms, systems, framework, techniques, system, models, machine, algorithm, model, technology, frameworks, based	" ,,, ', and, ., ", is, ",, "., for, ",, in, to,), ', -, with, (, ',, on, :, has,], \n,),, /, that, ") of,),, —, .', 's, as, at, can, ', ")
Natural Language	processing, interface, learning, understanding, based, programming, interfaces, generation, model, analysis	" ,, ., and, ",, "., -, .", ", is,), to, :, in, for, processor, ', (of, skills,),, \n, with, that, ;, ") as, ":", or,),, on, ,, processors, has, ") ,, "; can, at, /, by
Artificial Intelligence	Intelligence systems, research, technology, could, may	" ,, and, is, ., ", (, ., ", ., ', ", has, in, that, will, to, :, for,), \n, can, or,], as,),, -, —, —, /, with, ?, -,),, on, ;, 's, ', of, ', was, ") [at, -, ")